Chapter 5

Plasma transfer processes at the magnetopause

5.1. Introduction

With the possible exception of a small area at each of the two magnetic cusps, classical theory of interaction between the solar wind and the magnetosphere predicts the magnetopause to be an impenetrable boundary separating cold (~ 100 eV) dense ($\sim 30\,\mathrm{cm}^{-3}$) plasmas on magnetosheath magnetic field lines from hot (~ 1 keV) tenuous ($\sim 0.3\,\mathrm{cm}^{-3}$) plasmas on magnetospheric magnetic field lines. But in fact, observations indicate that a boundary layer of magnetosheath-like plasmas can be found just inside all regions of the magnetopause, including the nightside equatorial magnetopause (Hones *et al*., 1972), the low-latitude dayside magnetopause (Eastman *et al*., 1976; Haerendel *et al.*, 1978), and the high-latitude magnetopause (Rosenbauer *et al*., 1975; Paschmann *et al*., 1976). A recent statistical survey indicates that this layer is present on over 90% of all equatorial and mid-latitude magnetopause crossings (Eastman *et al*.,1996). The boundary layer is often divided into the low-latitude boundary layer (LLBL), the entry layer near the polar cusps, and the plasma mantle (PM) along the high-latitude magnetotail. Some reports suggest that such plasmas can be observed deep inside the magnetosphere during periods of strongly northward IMF orientation (Mitchell *et al*., 1987; Sauvaud *et al*., 1997; Fujimoto *et al*., 1997). These observations, together with numerous reports of a solar wind-like ion composition in magnetospheric plasmas (*e.g*., Sharp *et al*., 1974; Lennartsson and Shelley, 1986; Kremser *et al*., 1988a; Eastman and Christon, 1995), are evidence for the entry of magnetosheath plasma into the magnetosphere.

Low-altitude observations across the polar cap region suggest that the entry of magnetosheath plasma into the magnetosphere must be fairly widespread and rather continual. A fraction of the magnetosheath particles precipitate into the ionosphere immediately after they enter the magnetosphere, following the extension of the polar cusps to low altitudes, where they can be observed on more than 60% of spacecraft passes above the high-latitude dayside ionosphere (*e.g.*, Newell and Meng, 1992).

Similarly, observations of ionospheric ions outside the magnetopause pro-

vide evidence that magnetospheric plasma is also lost across the magnetopause (Peterson *et al.*, 1982; Fuselier *et al.*, 1995). Furthermore, energetic magnetospheric particles are a common feature outside both the dayside and nightside magnetopause (Meng and Anderson, 1970; West and Buck, 1976; Baker and Stone, 1977; Meng *et al.*, 1981). The chance of observing significant fluxes of energetic ($E > 15\,\mathrm{keV}$) magnetospheric ions just outside the dayside magnetopause exceeds 60% (Kudela *et al.*, 1992). The layer of magnetospheric particles outside the magnetopause is often referred to as the magnetosheath boundary layer (MSBL).

Since the processes allowing plasma to cross the magnetopause need not take place in the immediate vicinity of the spacecraft making the observation, these high rates of occurrence suggest that the solar wind-magnetosphere interaction never ceases, and that solar wind mass, energy, and momentum are constantly being transferred to Earth's magnetosphere. Estimates of the total amount of plasma entering the day-side magnetosphere and streaming tailward in the plasma mantle and LLBL are on the order of $10^{26}\,\mathrm{ions\,s^{-1}}$ (Hill, 1979; Eastman *et al.*, 1976). Observations within the magnetotail lobes indicate that plasma continues to enter the magnetotail throughout its entire length (*e.g.*, Gosling *et al.*, 1985).

A wide variety of processes have been proposed to account for the transfer of solar wind mass into the magnetosphere, and the escape of magnetospheric particles into the magnetosheath. This chapter addresses magnetic reconnection (Section 5.2), finite Larmor radius effects (Section 5.3), diffusion (Section 5.4), the Kelvin-Helmholtz instability (Section 5.5), impulsive penetration (Section 5.6), and direct cusp entry (Section 5.7). Our overall objective is to evaluate the significance of each of the aforementioned mechanisms to plasma transfer into and out of the magnetosphere. We begin by describing the basic physics underlying each mechanism, outline testable predictions from both theory and numerical simulations, and then describe the results of observations. As will be seen, the reconnection model has been developed to the point where it makes the greatest number of testable predictions, many of which have been confirmed by case and statistical studies. Nevertheless, the relative contribution of reconnection to the total amount of plasma entering and exiting the magnetosphere remains to be determined. We conclude the chapter with a summary (Section 5.8), followed by an outline of those theoretical and observational developments which are needed in the future (Section 5.9).

5.2. Magnetic Reconnection

5.2.1. INTRODUCTION

In Section 5.1 we defined the magnetopause as the boundary separating Earth's magnetic field and plasma from the interplanetary magnetic field and solar wind

plasma. This description is only valid within ideal MHD, where the magnetic field is frozen to the plasma. The frozen-in condition applies whenever the collision-free path is large compared with the dimensions of the system, which is generally true for the magnetospheric boundary region. It implies that the interplanetary magnetic field remains tied to the solar wind plasma, and Earth's magnetic field to the magnetospheric plasma, and the magnetopause is therefore an impenetrable boundary.

When the collisionless path length becomes sufficiently small somewhere within the magnetopause current layer for one reason or another, dissipation becomes important and the frozen-in condition may break down, allowing interplanetary and geomagnetic field lines to diffuse into that layer and become reconnected. Possible causes for this breakdown, and the resulting 'thawing' of the field lines (Scudder, 1997), are discussed in Section 5.2.2. Depending on the length of the X-line that exists at the centre of the diffusion region and the time-scale of the process that breaks the frozen-in condition, magnetopause reconnection may be large scale and quasi-stationary, or it may be patchy and transient. The latter situation is commonly thought to be the origin of the so-called 'flux transfer events'(FTEs), discovered by Russell and Elphic (1978).

The frozen-in condition remains a good approximation everywhere else, with the exception of regions where there are electric fields directed along the magnetic field, such as in the auroral acceleration region. Thus the newly reconnected flux tubes will become frozen into the plasma again, and maintain their interconnection, once they have left the diffusion region. Magnetosheath plasma can then simply flow along the magnetic field onto terrestrial field lines, thereby adding mass, energy and momentum to the magnetospheric plasma population. Likewise, magnetospheric particles can escape along field lines. This two-way transfer across the magnetopause continues while the flux tube convects tailward with the external plasma flow. Figure 5.1 schematically illustrates the geometry in the vicinity of the X-line.

Section 5.2.2 reviews the predictions of magnetopause reconnection models and their experimental tests. They are organised by scale, starting with 'microscale', proceeding to 'mesoscale', and ending with 'macroscale' predictions. Although the occurrence of reconnection depends critically upon the plasma behaviour *within* the diffusion region, essentially all of the experimental tests pertain to locations *outside* the diffusion region because observations within the reconnection region are not available (or have not been recognised as such).

When reconnection is occurring, the definition of the magnetopause becomes blurred, because it no longer strictly separates the geomagnetic and interplanetary fields and plasmas. However, because only a small fraction of the fields reconnects, the magnetopause generally remains a well-defined current sheet that can be identified by a change in magnetic field magnitude and/or direction, and a change in plasma properties.

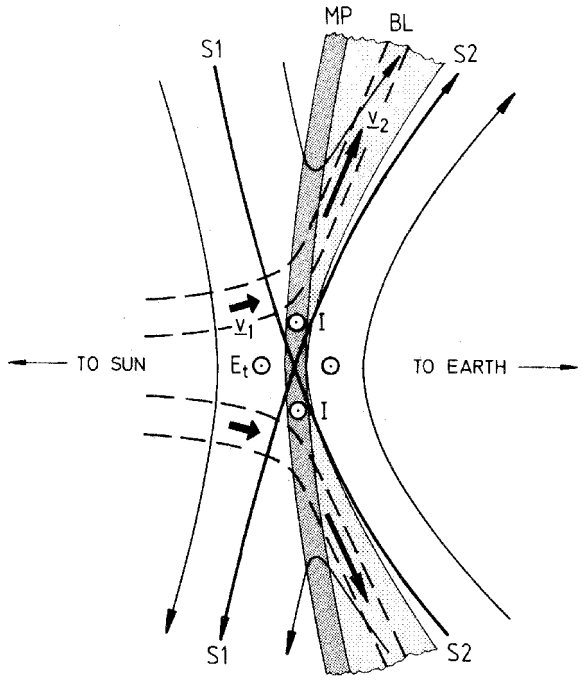

Figure 5.1. Meridional view of the reconnection configuration for antiparallel internal and external magnetic fields (after Sonnerup *et al.*, 1981). The magnetopause (MP) is shown as a current layer of finite thickness, with an adjoining boundary layer (BL) . The field lines connected to the separator (or X-line) are the outer (S1) and inner (S2) separatrix, respectively. They separate magnetic field lines with different topology. Dashed lines are stream lines and the heavy arrows indicate the plasma flow velocity. The reconnection electric field, $\mathbf{E}_t$, is aligned with the magnetopause current, **I**. The reconnection process occurs in an area of unknown dimension around the X, called the diffusion region.

5.2.2. THEORETICAL BACKGROUND

Morphology of Reconnection

A number of reconnection models have been developed. All these models assume the existence of a diffusion region where the frozen-in condition breaks down.

In the Sweet-Parker model of reconnection (Sweet, 1958; Parker, 1963) magnetic field reconnects in a diffusion region with a length l corresponding to the total system size. The reconnection rate is defined as the Alfvén Mach-number $M_A = v_{in}/v_A$ in the inflow region. In the Sweet-Parker model, it is found (see *e.g.*, Lee, 1995) that $M_A = R_m^{-1/2}$, where $R_m = \mu_0 L v/\eta$ is the magnetic Reynolds number, defined as the ratio of the typical bulk velocity, v, times characteristic length L of the variation in the magnetic field, and the magnetic diffusivity (see Appendix B), $D_m = \eta/\mu_0$. Because $R_m \gg 1$, the reconnection rate in the

Sweet-Parker model is rather small.

Petschek (1964) introduced the idea that the diffusion region is much shorter than the overall size l and that the outer region contains two pairs of standing slow mode shocks. These shocks deflect and accelerate the incoming plasma into two exit jets wedged between the shocks: acceleration is due to the Maxwell stress at the slow mode shocks. The maximum reconnection rate, based on parameters outside the diffusion region, is found to be $M_A = \pi/(8 \ln R_m)$, much larger than the Sweet-Parker rate and typically of the order 0.1. Sonnerup (1974) proposed a steady state reconnection model with slow mode expansion waves generated by corners in the inflow region. In this model the streamlines diverge as the plasma flows in. The divergence is due to a decreasing pressure; however, since the magnetic field simultaneously increases, the expansion is of the slow mode type.

Priest and Forbes (1986) derived a uniform model for steady-state reconnection. As in Petschek's model, the magnetic field and plasma velocity in the inflow region represent expansions about a uniform field and a plasma at rest. The Petschek solution, the Sonnerup solution, and the flux pile-up regime, are special cases of the generalised Priest-Forbes solution.

Levy *et al*. (1964) pointed out that reconnection between magnetic fields of different strength on both sides of the current sheet leads not to two symmetric slow mode shocks, but rather to a system of MHD waves standing in the flow downstream from the reconnection site. Five discontinuities are needed to match the upstream and downstream conditions: an Alfvén wave, a slow-mode shock, a contact discontinuity, another slow-mode shock, and another Alfvén wave (*e.g.*, Lin and Lee, 1993; Heyn, 1995). These discontinuities are located in the wedge between the two separatrices S1 and S2 shown in Figure 5.1. Observationally it is the outer Alfvén wave that is identified with the magnetopause.

Breaking the Frozen-In Condition

To gain insight into the processes causing breakdown of the frozen-in condition, consider the generalised Ohm's law. Assuming quasi-neutrality in two-fluid theory, the electric field is determined by the electron momentum equation

$$\mathbf{E} + \mathbf{v}_e \times \mathbf{B} = -\frac{1}{en}\nabla \cdot \mathsf{P}_e - \frac{m_e}{e}\frac{d\mathbf{v}_e}{dt} - \frac{m_e \nu_{ei}}{e}(\mathbf{v}_e - \mathbf{v}_i) \tag{5.1}$$

Here P_e denotes the full electron pressure tensor, n is the number density of both ions and electrons, $\mathbf{v}_e$ and $\mathbf{v}_i$ are the electron and ion bulk flow velocities, and ν_{ei} is the electron-ion collision rate. This equation can be rewritten in terms of the current $\mathbf{j}$ as

$$\mathbf{E} + \mathbf{v}_i \times \mathbf{B} = \frac{1}{en}\mathbf{j} \times \mathbf{B} - \frac{1}{en}\nabla \cdot \mathsf{P}_e + \frac{1}{\epsilon_0 \omega_{pe}^2}\frac{\mathrm{d}\mathbf{j}}{\mathrm{d}t} + \eta \mathbf{j} \tag{5.2}$$

where ω_{pe} is the electron plasma frequency.

While the left-hand side of Equation (5.2) describes the frozen-in state, the terms on the right-hand side refer to four different processes. The first term is the Hall term, the second term accounts for electron pressure effects, the third term is the electron inertial term, and the fourth term is the resistive term, with η the plasma resistivity. In the case of significant current flow, it is actually the left-hand side of Equation (5.1) that describes the frozen-in state, because the magnetic field is more closely tied to the electron fluid than to the ion fluid.

The relative importance of these terms (*cf. e.g.*, Drake, 1995) is related to four characteristic length scales, the electron skin depth, $\lambda_e = c/\omega_{pe}$, the ion skin depth, $\lambda_i = c/\omega_{pi}$, the effective ion Larmor radius, $r_{ci} = (k_{\rm B}T_e/m_i)^{1/2}/\omega_{ci}$, and the resistive scale length, $\Delta = \eta/\mu_0|\mathbf{v}|$. These terms are discussed separately below. The process with the largest scale length will dominate the breaking process.

The Hall term becomes important when the ion inertia length $\lambda_i = c/\omega_{pi} \sim \Delta$. In the diffusion region the ions are essentially unmagnetised while the magnetic field remains frozen into the electron fluid alone. Therefore, the Hall term in itself does not cause thawing in stationary reconnection. It does, however, modify reconnection. The influence of the Hall term on the reconnection rate has been investigated by Mandt *et al*. (1994) and by Lottermoser and Scholer (1997). In time-dependent reconnection it introduces whistler and kinetic Alfvén dynamics.

In 2-D, a scalar electron pressure or an electron pressure tensor with only diagonal elements does not lead by itself to a parallel electric field and also does not cause reconnection (Scudder, 1997). It can, however, drastically alter the mode of reconnection when the effective ion Larmor radius r_{ci} dominates. Kleva *et al*. (1995) performed 2-1/2 D simulations of reconnection retaining the pressure gradient term and taking into account a finite guide field in the invariant direction. They showed that this reduces the length of the current layer considerably and allows for a fast reconnection rate of the order of the Alfvén speed due to the fact that the pressure gradient balances the parallel electric field and no large parallel current is necessary.

When the classical resistivity is zero, electron inertia also enables the flux constraint to be broken and reconnection to proceed. Under these conditions, the reconnection electric field is supported by the term $1/(\epsilon_0\omega_{pe}^2)(\mathrm{d}\mathbf{j}/\mathrm{d}t)$. As can be seen from Ohm's law, electron inertia becomes important on scale-lengths comparable to the electron skin depth, $\lambda_e = c/\omega_{pe}$. When the resistivity, regular or anomalous, is finite, the frozen-in condition is broken by definition. In the case of a collisionless plasma such a resistivity may be provided by an instability, *e.g.*, by a current driven instability.

An important and unresolved issue concerns the size of the diffusion region. For collisionless reconnection, the thickness, d, is expected to lie somewhere between the electron and ion skin depths, *i.e.* $c/\omega_{pe} < d < c/\omega_{pi}$. Hence $1 < d < 50$ km for typical magnetopause conditions. The length along the magneto-

pause, *i.e.* in the direction tranverse to the X-line, is even more uncertain, but presumably larger than its thickness. For reconnection via anomalous resistivity, on the other hand, the length of the diffusion region is not constrained *a-priori*.

5.2.3. PREDICTIONS AND TESTS: MICROSCALE

In this section we describe predictions and tests pertaining to the magnetopause itself. Fluid and kinetic effects are discussed separately. Because we deal with tests outside the diffusion region, ideal MHD is the basis for the fluid description.

Ideal MHD

With the arrival of high time resolution ISEE-1 and -2 plasma and magnetic field data in the late 1970's, it became possible to apply the predictions of single-fluid anisotropic MHD theory to magnetopause current layer observations. Predictions for anisotropic MHD have been obtained under an assumption that the magnetopause is locally a one-dimensional rotational discontinuity whose properties remain steady on time scales long compared to the transfer of a single-fluid plasma element across the discontinuity.

Quantities Related to the Reconnection Rate. When reconnection occurs (*cf.* Figure 5.1), the tangential (t) and normal (n) components of the magnetic field ($\mathbf{B}$), velocity ($\mathbf{v}$), and electric field ($\mathbf{E}$) obey the following inequalities at the magnetopause:

$$B_n \neq 0, \qquad v_n \neq 0, \qquad |\mathbf{E}|_t \neq 0. \tag{5.3}$$

The ratios

$$M_{An} = v_n/v_A = B_n/|\mathbf{B}| \tag{5.4}$$

provide information concerning the reconnection rate and the transfer of mass across the magnetopause, where $v_A = B/\sqrt{\mu_0\rho}$ is the Alfvén velocity in the inflow region, and ρ is the mass density. Note that according to Eq. (5.4), the plasma flows across the magnetopause with a speed v_n that is proportional to the normal magnetic field strength, B_n, $v_n = B_n/\sqrt{\mu_0\rho}$.

Several case studies indicate that generally $M_{An} < 0.1$ (*e.g.*, Sonnerup and Ledley, 1979). Direct identification of a magnetic field component normal to the magnetopause ($B_n \neq 0$) in a background field $\mathbf{B}$ therefore requires knowledge of the magnetopause orientation to better than 6°. Minimum variance analysis of magnetic field data from a single spacecraft generally does not yield boundary normals with this accuracy. However, there have been occasional reports of non-zero normal components at the magnetopause (*e.g.*, Sonnerup and Ledley, 1979). Difficulties in identifying B_n suggest that the typical reconnection rate is less than 0.1.

Measuring v_n or $\mathbf{E}_t$ directly is even more difficult. Near the dayside magnetopause, v_A is typically of the order of 250 km s^{-1}. A reconnection rate of

$M_{An} \approx 0.1$ therefore requires the identification of a $v_n \approx 25\,\mathrm{km\,s^{-1}}$ flow normal to the magnetopause in a region where background tangential flow velocities typically range from $\mathbf{v}_t \approx 100$ to $250\,\mathrm{km\,s^{-1}}$. Furthermore, the velocity component normal to the magnetopause must be measured in the rest frame of the magnetopause. Statistical surveys reveal that the magnetopause is constantly in motion with radial velocities typically of the order of 20 to $30\,\mathrm{km\,s^{-1}}$ (Phan and Paschmann, 1996). Because observed velocities are almost always consistent with the sense of boundary motion (*e.g.*, earthward velocities are associated with crossings from the magnetosphere to magnetosheath), v_n at the magnetopause must in fact be substantially smaller than $v_n < 25\,\mathrm{km\ s^{-1}}$. There are similar difficulties identifying non-zero tangential electric fields because the dominant component is directed normal to the magnetopause.

In summary, non-zero normal components of the magnetic field and plasma velocity, and tangential components of the electric field are fundamental predictions of MHD theory. Although they provide one of the few direct measures of the reconnection rate, they are usually too small to measure, indicating that reconnection rates are typically less than 0.1.

Existence of an HT Frame. The existence of a magnetic field component normal to the magnetopause requires magnetic field lines on both sides of the discontinuity to move together. If so, there must be a reference frame in which the flow (as well as any electric field component) are field-aligned on both sides of the discontinuity. This deHoffmann-Teller (HT) reference frame slides along the discontinuity with the 'field-line velocity', $\mathbf{v}_{\mathrm{HT}}$, *i.e.* the velocity with which interconnected field lines that thread the surface of the discontinuity move along the layer. The existence of a HT frame is thus a necessary (but not a sufficient) condition for identifying an open magnetopause and ongoing reconnection.

Tangential Stress Balance. As a result of the tangential Maxwell stress at a discontinuity with a normal magnetic field component (rotational discontinuity, RD), the tangential momentum of the magnetosheath plasma changes from one side to the other. For a current layer that is locally one-dimensional and stationary, this can be expressed by the relationships (Hudson, 1970):

$$\mathbf{v} - \mathbf{v}_{\mathrm{HT}} = \pm \mathbf{v}_{\mathrm{A}} \tag{5.5}$$

$$\rho(1-\alpha) = \mathrm{const} \tag{5.6}$$

where $\alpha = (p_{||} - p_{\perp})\mu_0/B^2$ is the pressure anisotropy factor and $\mathbf{v}_A$ is the intermediate mode wave velocity $\mathbf{v}_{\mathrm{A}} = \mathbf{B}[(1-\alpha)/\mu_0\rho]^{1/2}$ corrected for pressure anisotropy. The choice of sign in Eq. (5.5) (often referred to as the Walén relation) depends on whether the flow is parallel or antiparallel to the magnetic field, or equivalently whether the observations are made north or south of the location of

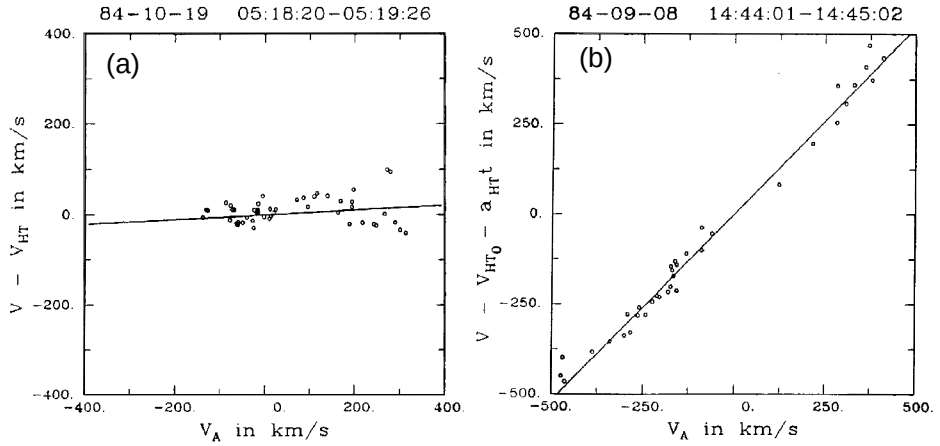

Figure 5.2. Walén test for two magnetopause crossings by the AMPTE/IRM spacecraft. Plotted are the three components of the plasma velocity in the HT frame versus the corresponding components of the Alfvén velocity. In example (b), on the right, the points fall along the diagonal, implying good agreement with the Walén relation (5.5). The positive slope indicates a crossing northward of the X-line, where B_n is pointing inwards. (To improve the agreement, the HT frame was assumed to be accelerating in this case). By contrast, example (a), on the left, shows a crossing where the Walén relation is not satisfied, implying that the magnetopause was a tangential discontinuity in this case (from Sonnerup *et al*., 1990).

the X-line where reconnection occurs at the magnetopause (*cf.* Figure 5.1). For further discussion see the review by Sonnerup *et al*. (1995).

The Walén relation states that in the HT frame of reference the plasma flow is alfvénic. Figure 5.2 shows experimental tests of the relation for two magnetopause crossings by the AMPTE/IRM spacecraft. The example on the right shows nearly perfect agreement, indicating that the magnetopause crossing occurred at a location where the magnetic fields were interconnected across the magnetopause. In the example on the left there was total disagreement with the Walén relation, indicating a crossing where the fields were not interconnected, at least not at the location of the crossing.

If measurements are considered in the laboratory (or spacecraft) frame, Eq. (5.5) predicts a change in flow velocity across the magnetopause that is equal to the change in Alfvén velocity

$$\Delta \mathbf{v} = \pm \Delta \mathbf{v}_A \tag{5.7}$$

Although not explicitly appearing in the equations, it is the tangential electric field, $\mathbf{E}_t$, implied by reconnection (*cf.* Figure 5.1) that is responsible for the acceleration of the plasma in the spacecraft frame. While crossing the magnetopause, particles are displaced along the magnetopause surface such that the change in

energy from the tangential electric field satisfies Eq. (5.7). Note that for a tangential discontinuity, the velocity jump across the discontinuity is arbitrary and thus can only accidentally satisfy Eq. (5.7).

Near the subsolar magnetopause, where the magnetosheath flow speed is small ($v \approx 100\,\mathrm{km\,s^{-1}}$ or less), but the change in Alfvén velocity across the magnetopause can become large, Eq. (5.7) predicts flow speeds inside the boundary layer that can become as high as $\approx 500\,\mathrm{km\,s^{-1}}$. It was in this region that the first successful tests of Eq. (5.5) were carried out (Paschmann *et al.*, 1979, Sonnerup *et al.*, 1981). These high-speed flow ('plasma jetting') cases were considered the first strong *in situ* evidence for reconnection at the magnetopause.

Many comparisons have since been made, using nearly 50 ISEE magnetopause crossings (summarised by Sonnerup *et al.*, 1995) and 69 AMPTE/IRM crossings (Phan *et al.*, 1996) where the magnetic field shear across the magnetopause was large, *i.e.* reconnection could be expected to occur. In about half the cases the observed flow velocities did obey Equation (5.7) reasonably well. This might imply that at the time and location of the other half of these crossings the magnetic fields were not interconnected across the magnetopause. But experimental errors may also have contributed. Among these are the lack of ion-mass-resolution and limited temporal resolution of the measurements. When applying Equation (5.5), errors are also introduced by taking the ion bulk velocity to determine the HT frame (in lieu of direct electric field measurements) rather than the electron bulk velocity, although the magnetic field is more closely tied to the electrons than to the ions. Needless to say, the assumptions underlying the application of Equation (5.5) or (5.7), namely time-stationarity and one-dimensionality, could equally well be violated at the magnetopause and thus cause discrepancies between predictions and observations. The fact that measured flow speeds are almost always less than those predicted probably cannot be explained by experimental errors. Reasons for this have been suggested (Sonnerup *et al.*, 1995; Phan *et al.*, 1996), but there has been no final resolution.

Note that in the above tests, a variant of Equation (5.7) was actually employed that utilises Equation (5.6) to express the change in mass density by the change in anisotropy, because the measurements did not resolve ion mass. So the validity of Equation (5.6) was *assumed* in the analysis. Actually testing this equation requires measuring the velocity space distributions for the major ion species. To date, the composition measurements have been made at a time resolution considerably less than that for non-mass resolving ion instruments. Nevertheless, Fuselier *et al.* (1993) attempted to test Equation (5.6) using AMPTE/CCE data. They confirmed that solar wind H^+ dominates magnetopause plasma populations. Their results suggest that Equation (5.6) does not hold across the magnetopause. These results have been challenged on the basis of the instrumental time resolution (*cf. e.g.*, Sonnerup *et al.*, 1995).

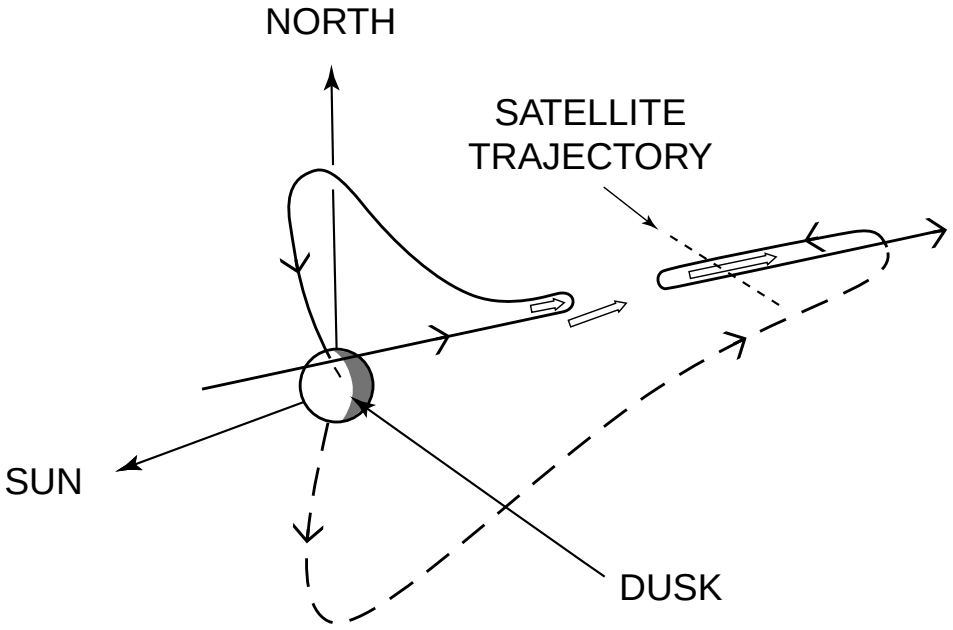

Figure 5.3. Sketch illustrating reconnection of a magnetosheath field line with a field-line from the near-tail plasma sheet (from Gosling *et al*., 1986).

In regions where the magnetosheath flow speed is comparable to or larger than the Alfvén speed (*i.e.* further away from the subsolar region), Equation (5.7) still predicts an acceleration of the flow, but not necessarily an increase in speed (Scudder, 1984; Cowley and Owen, 1989). But even at the dusk flank of the magnetopause, high-speed flows satisfying Eq. (5.7) have been observed (Gosling *et al*., 1986). Figure 5.3 illustrates the geometry inferred for reconnection at the dusk flank of the magnetopause. RD identifications have also been made at the magnetopause even further down the magnetotail (Sanchez et al., 1990). Note that reconnection should cease to operate if the velocity in the adjacent magnetosheath becomes too large (La Belle-Hamer *et al*., 1995).

An important consequence of the curvature forces resulting from the sharp bends in reconnected field lines is that they can be strong enough to reverse the plasma flow direction upon entry from the magnetosheath to the LLBL, as has been demonstrated by the observations reported by Gosling *et al*. (1990a).

When the observations satisfy Equation (5.5) (or 5.7), the sign on the right-hand side of the equation is fixed. The sign in turn determines on which side of the X-line the measurement was made. Thus each observation sets a limit on the location of the X-line. For example, a crossing at northern latitudes that, based on the observed sign in Equation (5.5), is identified as a crossing north of the X-line, obviously implies that the X-line is located south of the crossing, possibly at

low latitudes. A crossing at the same northern latitude, but with flows implying a crossing south of the X-line, definitely requires the X-line to be at high northern latitudes. From their composite of observations, Phan *et al*. (1996) concluded that the X-line location is not constrained to low latitudes.

Few observations of plasma flows have been made in the cusp regions that would be suitable for the identification of reconnection expected to occur at times of northward IMF. Important exceptions are a few cases of a flow reversals observed in high-latitude magnetopause crossings (Gosling *et al*., 1991; Kessel *et al*., 1996).

Finally, note that the underlying assumptions of one-dimensionality and stationarity usually prevent the application of the Walén test to FTEs. This lack of a quantitative test is one reason why the explanation of FTEs in terms of localised transient reconnection is not straightforward.

Kinetic Effects

The predictions listed above were for a single-fluid plasma. In reality, the magnetosheath and magnetosphere plasmas should be described as multi-fluids. There are no equivalent stress balance predictions for multi-fluids. Thus, for example, Equation (5.5) is really a test for the centre of mass of the multi-fluid plasma. For most cases at Earth's magnetopause, the centre of mass of the multi-fluid plasma corresponds to that for the dominant magnetosheath H^+ distribution. To make predictions for individual ion species, we must consider the motion of single particles. Once again, it becomes important to assume the existence of a HT reference frame. This assumption forces the flow velocities of the individual ion species perpendicular to the magnetic field to be identical. If this were not the case, the differing ion species would drift across the magnetic field and there would be no reference frame wherein the electric fields associated with the individual ion species vanished on either side of the discontinuity. Because of the limited number of magnetopause observations with full composition measurements, the perpendicular flow velocities of individual ion species at the magnetopause have been compared only for a small number of magnetopause crossings. In general, good agreement is found for low latitude magnetopause crossings (Paschmann *et al*., 1989; Gosling *et al*., 1990a; Fuselier *et al*., 1993). Observations at high latitude magnetopause crossings show substantially less agreement with predictions (Lundin *et al*., 1987). Reconciling the high and low latitude observations remains an open issue.

Flow behaviour and particle distributions can be predicted from a kinetic treatment of individual particles in the HT frame (*cf. e.g.*, Cowley, 1982; Sonnerup, 1984). In the HT frame, there is no electric field and the particles conserve total energy while moving along the magnetic field from the magnetosheath into the LLBL. The kinetic energy changes in the HT frame when there is an intrinsic potential difference across the magnetopause, but presently there is no evidence

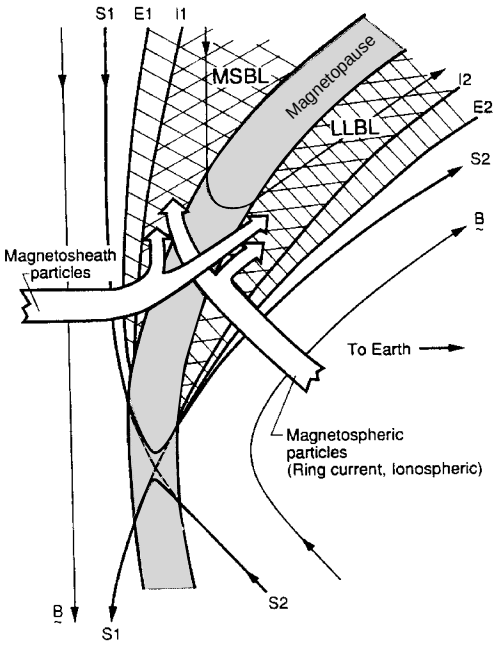

Figure 5.4. Qualitative sketch of the magnetopause region for quasi-stationary reconnection. Magnetosheath ions either reflect off the magnetopause and enter the MSBL, or cross the magnetopause and enter the LLBL. Conversely, magnetospheric ions either reflect off the magnetopause and enter the LLBL, or cross the magnetopause and enter the MSBL (from Gosling *et al*., 1990b).

that such intrinsic potentials exist.

It is also usual to assume that the particles' pitch angles remain unchanged or else that they all change by an equal amount across the boundary. Since there is no electric field, all ions starting out in the magnetosheath with equal velocities have equal velocities once they cross the magnetopause. Thus, assuming adiabatic motion of the individual ions across the magnetopause and realising that the H^+ and He^{+2} distributions have similar flow velocities in the magnetosheath, the theory predicts equal flow velocities parallel to the magnetic field in the LLBL for H^+ and He^{+2}. Paschmann *et al*. (1989) and Fuselier *et al.* (1993) report several magnetopause crossings consistent with this prediction.

If it is further assumed that particles either reflect at or cross the magnetopause (Figure 5.4), then detailed distribution functions can be predicted near the boundary (Cowley, 1980; see also Cowley, 1995). In particular, only those ions with velocities in excess of a threshold determined by the HT frame will be able to cross the boundary and enter either the magnetosheath boundary layer (MSBL) or the LLBL (Figure 5.5).

This leads to the prediction of so-called 'D-shaped' distributions for ions crossing the boundary. Such distributions have been observed in the LLBL (*cf.*

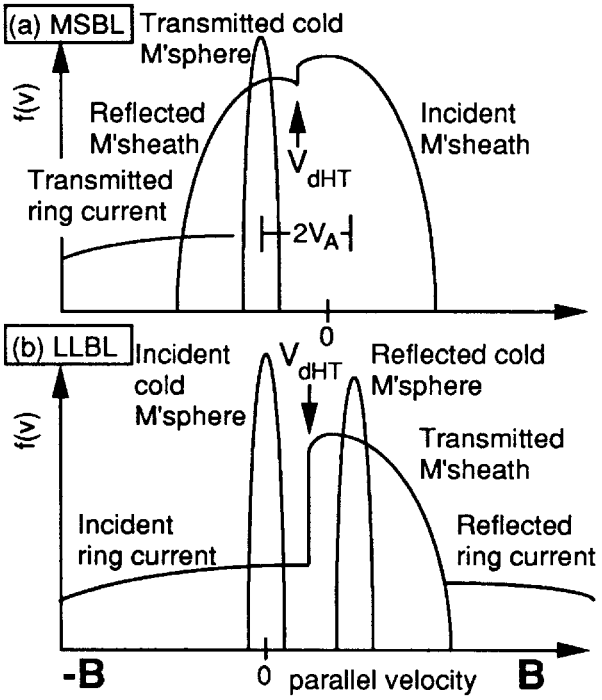

Figure 5.5. Qualitative sketch of the ion distributions expected in the MSBL (a) and the LLBL (b) for a magnetopause crossing north of the reconnection line. If v_{HT} is small and the magnetosheath temperature is large, then the incident and reflected magnetosheath distributions in the MSBL will not be distinguished. Reflection will be difficult to observe in the LLBL because the transmitted sheath distribution dominates there (from Fuselier, 1995).

e.g., Smith and Rogers, 1991; Fuselier *et al.*, 1991). Furthermore, there should be reflected ions (and electrons) in the layers adjacent to the magnetopause (Figure 5.5).

Such ion reflection at the magnetopause has only rarely been reported in the literature (Scholer and Ipavich, 1983; Fuselier, 1995), probably due to the specific conditions characterising that boundary. One example is shown in Figure 5.6. When the component of the HT-velocity parallel to the magnetic field is small compared to the thermal speed of the incident solar wind distribution, it becomes difficult to distinguish incident and reflected distributions at the magnetopause. The large thermal speeds of incident magnetosheath distributions in the subsolar magnetosheath usually limit observation of reflected particles to cases in which the HT-velocity exceeds several hundred $\mathrm{km\,s^{-1}}$. For lower HT velocities, the incident and reflected distributions merge and can be misinterpreted as parallel heating in the MSBL. This is particularly true for magnetosheath electrons, which always exhibit thermal speeds on the order of $1000\,\mathrm{km\,s^{-1}}$.

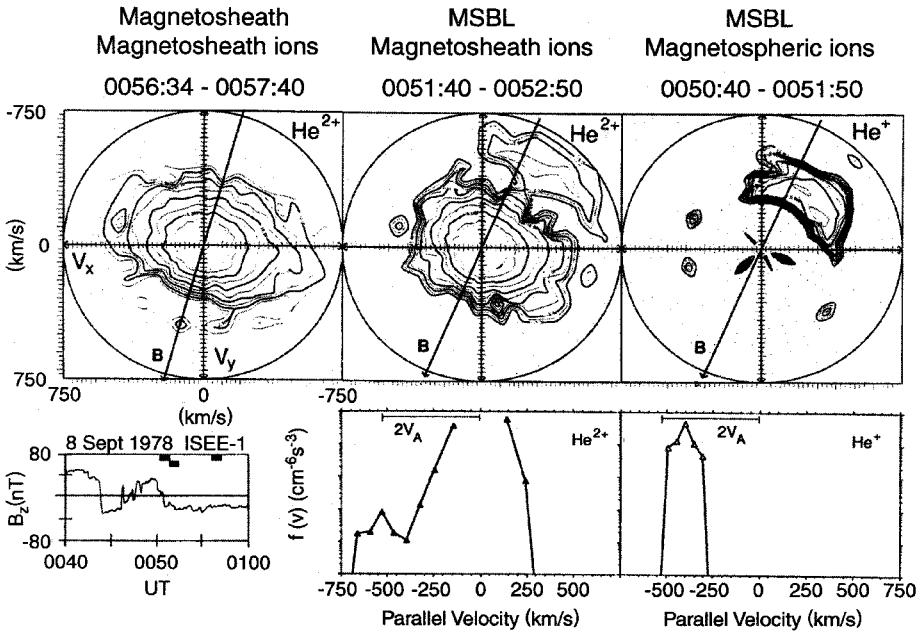

Figure 5.6. An example of ion reflection and transmission in the MSBL. The upper panels show phase space density contours in two-dimensional velocity-space and the lower panels show B_z and parallel cuts through the distributions. The intervals marked by black bars in the B_z trace show where the distributions have been measured, indicating that all three were measured on the magnetosheath side. The He^{+2} distribution near $V = 0$ in the first two panels is the incident magnetosheath distribution. The second distribution in the middle panel at $2V_A$ along B is the reflected magnetosheath distribution. Concurrent with this reflected distribution is the He^{+} distribution shown in the third panel which is the transmitted magnetospheric distribution (from Fuselier, 1995).

For conditions near the subsolar magnetopause where the flow tangential to the magnetopause is small and H^+ dominates the plasma, the spacecraft frame of reference is nearly the same as the plasma rest frame. Typically, low energy magnetospheric ions also have very low tangential velocities in the subsolar region. Under these restrictive conditions, individual ion populations should exhibit Alfvénic flow on both sides of the magnetopause in the HT frame. Thus, the incident and reflected components on both sides of the magnetopause should be separated by $2\mathbf{v}_A$ and the transmitted components on both sides should have velocities $\mathbf{v}_A$. Only a few magnetopause crossings have been investigated in such detail. The transmitted components have velocities somewhat less than predicted, while the reflected components on either side of these magnetopauses have velocities of $2\mathbf{v}_A$ (Fuselier *et al.*, 1991, Fuselier, 1995). Thus the kinetic test for individual components of the plasma confirms the results for a single fluid.

Reconnection models make no quantitative predictions for the reflection coefficients at the magnetopause. Recent observations indicating that the He^{+2}/H^+

plasma density ratio decreases by 40% from the magnetosheath to the LLBL, are thus not explained in the reconnection framework, and simply suggest that the reflection coefficient is mass dependent (Fuselier *et al.*, 1997a). A mass dependent reflection coefficient could be important for magnetospheric losses as well, especially for heavy ions in the magnetosphere. Incidentally, this decrease contradicts expectations based on entry via finite Larmor radius effects (*cf.* Section 5.3).

Finally, it should be noted that although reconnection signatures in the distribution functions are sometimes observed together with the fluid signatures, more often one signature is observed without the other (Bauer *et al.*, 1998). This fact is presently not understood.

5.2.4. PREDICTIONS AND TESTS: MESOSCALE

The previous section presented microscale predictions from single fluid MHD and kinetic theory. This section builds upon those results to make predictions at locations removed from the magnetopause boundary.

MHD Models

Two-dimensional MHD problems can be simplified by assuming that one of the coordinates is related to time by a convection velocity. For the MHD system with seven quantities ($B_y, B_z, \rho, P, v_x, v_y, v_z$), there are seven discontinuities across a current sheet. Two of these discontinuities are fast mode waves which convect rapidly away. The magnetopause and associated boundary layers therefore contain five discontinuities: two rotational intermediate modes, two slow modes, and one contact discontinuity. One or more of the seven quantities change at each discontinuity in the transition from the magnetosheath to the magnetosphere. There have been some attempts to identify these discontinuities at the magnetopause (Rijnbeek *et al.*, 1989; Bachmaier, 1994; Walthour *et al.*, 1994), but only one possible identification of the slow-mode wave has been made. The outer of the two intermediate-mode waves, on the other hand, has been identified frequently. It is this discontinuity across which the tangential stress balance tests described in the previous section have been carried out.

It should not be surprising that there has been little success identifying the various discontinuities at the magnetopause. Some of the five discontinuities mentioned above may be weak or become merged depending on initial conditions. Furthermore, kinetic simulations show that the contact discontinuity disappears and that the other discontinuities change characteristics (Lin and Lee, 1993; Omidi and Winske, 1995).

Kinetic Models

Microscale kinetic models provide another starting point for mesoscale predictions. Figure 5.7 shows the distinction between microscale and mesoscale tests of

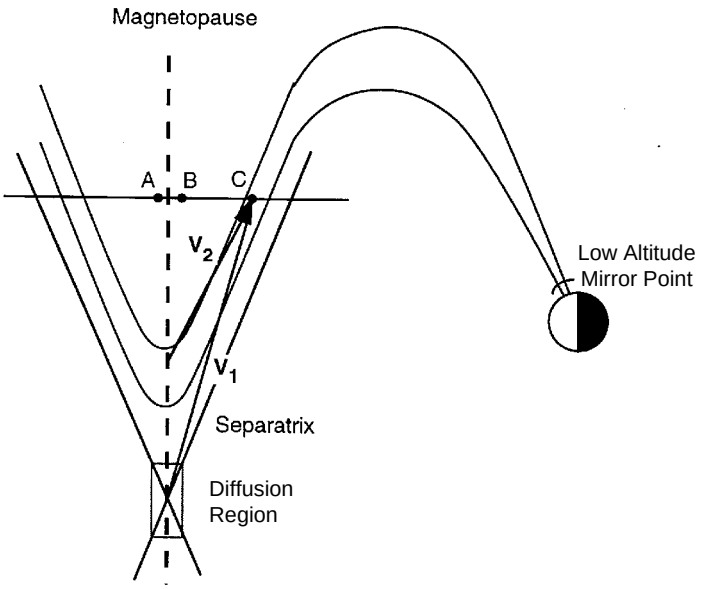

Figure 5.7. Microscale and mesoscale predictions at the magnetopause. For microscale predictions (between points A and B), the properties of the discontinuity are important. For mesoscale predictions (between A and C), one must take into account the finite extent of the reconnection region (velocity filter) and the presence of a low altitude mirror point. At point C ions and electrons can arrive from a region extending from the X-line to the location where the field line passing through C intercepts the magnetopause. The highest-energy ions and electrons (those with velocity v_2) arrive at point C from a location on the magnetopause close to the observation point. Ions and electrons crossing the magnetopause at this point with velocities $v < v_2$ cannot reach point C because there is insufficient time for them to move along the magnetic field line from the magnetopause to point C. The lowest-energy ions and electrons arrive at point C with velocity v_1 from the point on the magnetopause near the intersection of the separatrices. These ions and electrons are moving with the convecting field lines at velocity $v_1 = v_{\mathrm{HT}}$ in the rest frame of the magnetopause. Ions and electrons with velocities $v < v_{\mathrm{HT}}$ do not cross the magnetopause (figure provided by S. Fusilier).

reconnection at the magnetopause. Whereas microscale predictions relate conditions at two points immediately adjacent to the magnetopause (*i.e.* between points A and B), mesoscale predictions relate observations made further from the magnetopause (*i.e.* between points A and C). Mesoscale predictions must take into account the fact that the extent of the reconnection region is limited in one direction by the convergence of the separatrices in the diffusion region and the fact that the particles moving along the magnetic field lines can be reflected at a low altitude ionospheric mirror point.

Simple kinematics allows specific predictions for particle distributions in the vicinity of the magnetopause. One obvious prediction from the previous section is that ions and electrons are reflected and transmitted at the magnetopause. These reflected and transmitted particles produce layers on either side of the

magnetopause which have some features consistent with the kinetic considerations described in the previous section. Electrons are convenient tracers of field line topology because of their high speeds. The heat flux associated with escaping magnetospheric electrons should be a particularly good tracer of the magnetosheath magnetic field lines connected to the magnetosphere and ionosphere (*i.e.* at point A within the magnetosheath boundary layer in Figure 5.7), because there are no mirror points in the magnetosheath (Scudder *et al*., 1984). Several papers report observations of this heat flux, whose detection appears to depend upon the magnetosheath electron temperature (Fuselier *et al*., 1995, 1997b; Nakamura *et al*., 1997).

Kinetic mesoscale predictions go well beyond electron topology considerations. The predictions near the magnetopause discussed in the microscale section and simple kinematics in the boundary layers permit predictions of the detailed velocity space distribution functions at remote locations. In turn, remote observations of velocity space distribution functions provide important information concerning the properties of reconnection, including its location and variability, as well as plasma properties in the immediate vicinity of the reconnection site. The discussion of these mesoscale predictions begins with the distinctive distribution functions produced primarily by the velocity filter effect. The discussion is limited to southward IMF conditions, when reconnection is expected in the subsolar region. The macroscale section removes these limitations in order to consider reconnection over all regions of the magnetopause for all IMF conditions.

Velocity Filter Effect. The velocity filter effect results when plasma streams away from a spatially limited source in the presence of an electric field transverse to the magnetic field. Figure 5.7 illustrates this for one observation point and for reconnection occurring on the dayside magnetopause.

Because the typical thermal velocity of electrons in the LLBL (~ 1400 km s^{-1}) greatly exceeds that of ions (~ 400 km s^{-1}), one expects to observe reflected/transmitted electrons deeper inside the magnetosphere than ions. Thus, an important mesoscale prediction for reconnection at the magnetopause is the existence of a distinct electron layer near the separatrices, as illustrated in Figure 5.4. Gosling *et al*. (1990b) reported observations of such a layer at the inner edge of the LLBL, whereas Nakamura *et al*. (1996) reported corresponding observations of the layer at the outer edge of the magnetosheath boundary layer (MSBL).

Predictions for the detailed velocity space distributions observed within the LLBL also require consideration of effects associated with a low altitude mirror point, as illustrated in Figure 5.8. This figure shows the locations of magnetosheath particles on reconnected field lines at three sequential times.

The distribution displayed in the lower right of the figure shows a number of key predictions for mesoscale reconnection. First, the spacecraft measures magnetosheath plasma flowing both directions with respect to the ambient magnetic

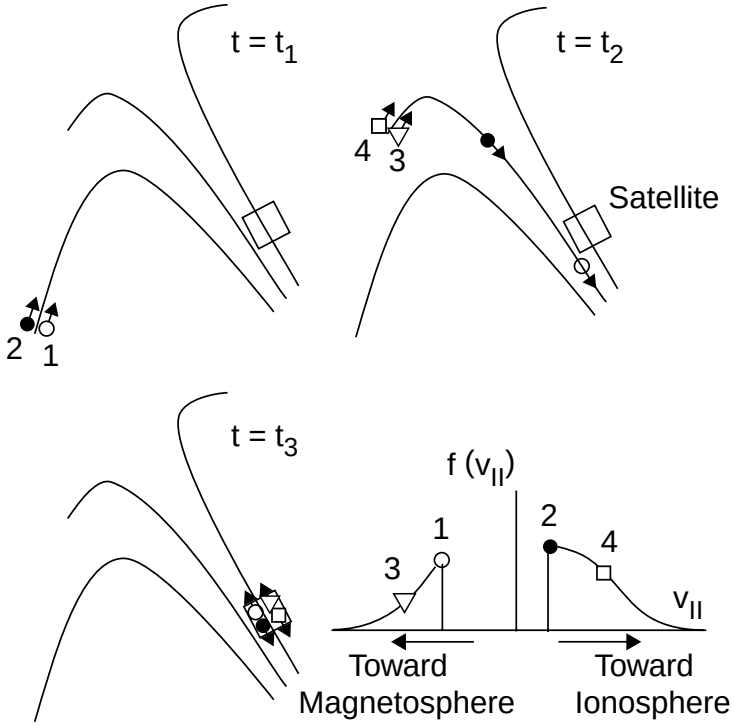

Figure 5.8. Effect of the low altitude mirror point on the velocity distribution of ions at the magnetopause. The upper left panel shows magnetosheath plasma entering the magnetosphere at time $t = t_1$, just as the flux tube reconnects. The open circle labelled (1) indicates a high velocity particle, the full circle (2) a low velocity particle. A short time later, at $t = t_2$, the flux tube has convected poleward in the presence of the dawn-dusk electric field, as shown in the upper right panel. By this time, particles with low velocities have travelled some intermediate distance into the magnetosphere whereas the particles with high-velocities have reached low altitudes. Magnetosheath plasma continues to enter the magnetosphere as the magnetopause crossing point of the open flux tube convects away from the reconnection site. Two additional particles cross the magnetopause at $t = t_2$: one with high velocity (3) and one with low velocity (4). The four velocities have been chosen such that at some later time, $t = t_3$, all are observed simultaneously by a spacecraft located above the ionospheric mirror point in the magnetosphere, as shown by the square in the lower left panel. The lower right panel illustrates the distribution function observed by the spacecraft at $t = t_3$ (figure provided by T. Onsager).

field. Some particles arrive directly from the magnetopause, whereas others have mirrored at low altitudes and are returning to the magnetopause. For both of these plasma components, there will be a low-speed cutoff, *i.e.* a velocity below which no magnetosheath plasma can be observed. The particles at these low-speed cutoffs are those that crossed the magnetopause when the field line first reconnected. The low-speed cutoff on the plasma component that has mirrored at low altitudes and is returning to the magnetopause will occur at a higher velocity than the directly entering component, since the mirrored component had to travel

a longer parallel distance to reach the spacecraft in the time since the flux tube reconnected.

Typically, ion velocities are comparable to the convection velocity of the field lines so that it takes many minutes for magnetosheath ions to propagate to the ionosphere, mirror and return to the magnetopause. In contrast, the high parallel speeds of the electrons allow them to propagate to the ionosphere, mirror, and return in time scales on the order of seconds. Thus, mirrored electrons should be more common. These mirrored electrons also exhibit the predicted higher velocity cut-offs (*cf. e.g.*, Gosling *et al*., 1990b).

On the basis of the velocity filter effect and ionospheric mirroring, it can be concluded that the observation of a broad distribution of velocities in the LLBL, cusp, and mantle is consistent with a spatially extended particle source region, *i.e.* the open magnetopause, and that the low-speed cutoff observed in these distributions is due to an edge in the open field lines that have access to a given location, *i.e.* a reconnection site.

In addition, the velocity filter effect predicts a dispersion of magnetosheath particles by energy versus latitude in the cusp and mantle. This feature is most pronounced and very common in proton measurements (*cf. e.g.*, Reiff *et al*., 1977), but it also occurs in precipitating solar wind He^{+2} ions (*cf. e.g.*, Fuselier *et al*., 1997b). Figure 5.9 shows a time sequence of proton distribution functions illustrating the energy-latitude dispersion and the evolution in the low-speed cut-off (Lockwood *et al*., 1994). In this example, the spacecraft travelled sunward at low altitudes across the polar cap, moving from field lines that had been interconnected for a long time into field lines that had been interconnected for a shorter time. Consequently, low energy protons were detected initially but were absent in later measurements. The characteristic evolution from higher to lower particle velocities has also been observed directly in traversals of the high-latitude magnetopause by Heos 2 that led to the discovery of the plasma mantle (Rosenbauer *et al*., 1975).

As mentioned above, reconnection predicts low-energy cut-offs in the spectra of injected magnetosheath particles observed at points removed from the magnetopause. Particles with energies just above the cut-off crossed the magnetopause at the initial moment and location of reconnection. By summing the fluxes of field-aligned particles at various points along the edge of the dispersion ramp, cutoffs at various energies are sampled and the distribution function of field-parallel particles near the reconnection site can be built up. Lockwood *et al*. (1994, 1995) have shown that these predicted distributions are consistent with the distribution functions of injected ions seen at the dayside magnetopause (*cf. e.g.*, Fuselier *et al*., 1991). This agreement confirms the validity of the underlying reconnection hypothesis.

Estimating the Distance to the Reconnection Site. In quasi-steady reconnection, the low-speed cut-offs on the measured distribution functions provide a means of

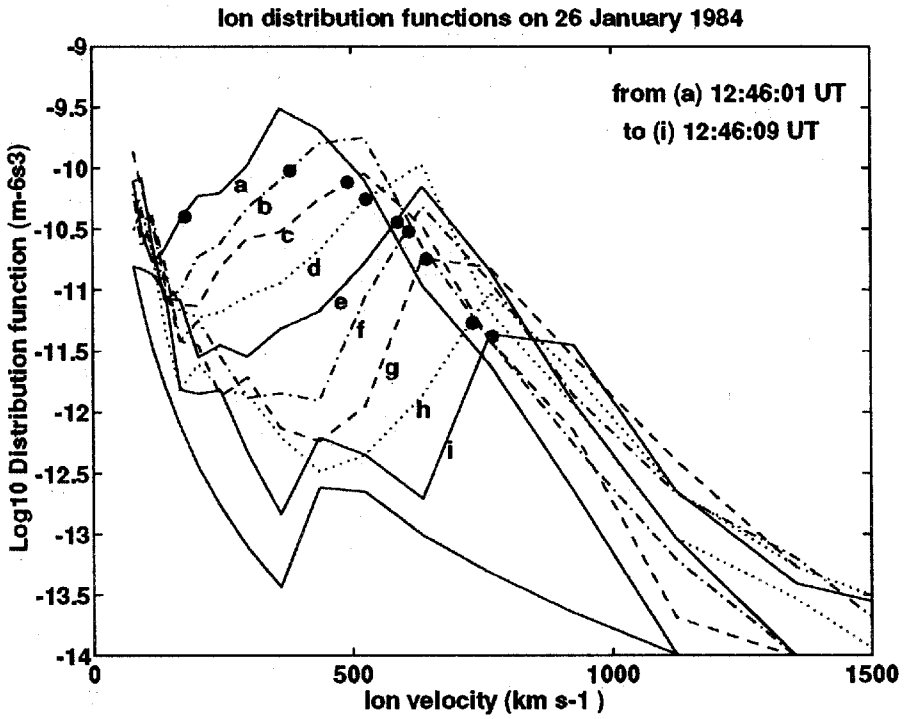

Figure 5.9. Time sequence of proton distributions showing energy-latitude dispersion measured on an equatorward pass through the low-altitude cusp (from Lockwood *et al*. 1994).

estimating the field-aligned distance from the spacecraft to the reconnection site (Onsager *et al*., 1990). As noted earlier, the low-speed cut-off on the mirrored population occurs at a higher velocity than that for the directly entering population. The relationship between the distance to the reconnection site and the two low-speed cut-offs is given by

$$\frac{d_r}{d_i} = \frac{2v_{lci}}{v_{lcm} - v_{lci}} \tag{5.8}$$

where d_r and d_i are the distances from the spacecraft to the reconnection region and the ionospheric mirror point, respectively, and v_{lci} and v_{lcm} are the low-speed cut-offs on the components flowing toward the ionosphere and the magnetosphere, respectively.

This formula has been applied to electron measurements in the LLBL (Gosling *et al*., 1990b), ion measurements in the LLBL (Fuselier *et al*., 1993, Onsager and Fuselier, 1994), electron measurements in the plasma sheet boundary layer (PSBL) (Onsager *et al*., 1990), ion measurements in the cusp (Phillips *et al*., 1993), and ion measurements in the PSBL (Elphic *et al*., 1995). Obviously, difficulties in identifying the low-speed cut-offs can lead to large uncertainties in the

estimates of the reconnection site location. Inferred locations of the reconnection site are quite variable. While some are consistent with the high-latitude magnetopause (summarised by Sibeck and Newell, 1994), others require a location in the subsolar region (*e.g.*, Sonnerup *et al*., 1981; Nakamura *et al*., 1996).

Estimating Variations in the Reconnection Rate. There are good reasons to believe that the location and rate of reconnection on the dayside magnetopause are constantly varying. Variations in the location and rate of reconnection would be expected to produce corresponding effects in the patterns of precipitating particles within the cusp and mantle. Here only reconnection variability is considered.

Pulsed reconnection causes abrupt steps in cusp ion precipitation cut-offs. Lockwood and Smith (1994) noted that the key factor in predicting these steps is the ratio of the spacecraft and convection velocities (v_s/v_c) in the direction normal to the boundary. Several non-steady cusp spectra features provide evidence for a series of short (< 1 min) reconnection bursts roughly separated by 10 min (Lockwood and Smith, 1992; Lockwood *et al*., 1995). Analysis of a large number of low-altitude cusp spectra indicates that the reconnection rate may be highly variable, even for seemingly steady-state cusp dispersion ramps (Lockwood *et al*., 1994), yet it rarely ceases for longer than about one minute, provided conditions at the magnetopause favour reconnection (Newell and Meng, 1995).

5.2.5. PREDICTIONS AND TESTS: MACROSCALE

Macroscale predictions concern the spatial and temporal occurrence of reconnection on the magnetopause as a function of varying solar wind conditions. The location and occurrence of reconnection directly determine when and where magnetosheath-like plasma can be observed inside the magnetosphere, and whether the plasma is observed steadily or in bursts.

Spatial Considerations

Concerning the location of the reconnection site, several models have been developed. Crooker (1979) and Luhmann *et al*. (1984) suggested that reconnection occurs when and where antiparallel magnetosheath and magnetospheric magnetic field lines come into contact. Consequently, they predicted reconnection with closed magnetospheric magnetic field lines on the dayside equatorial magnetopause when the IMF has a southward component, but with open lobe magnetic field lines on the polar magnetopause when the IMF has a northward component.

Other models require reconnection to occur along a subsolar line whose tilt depends upon the IMF orientation (*cf. e.g.*, Sonnerup, 1974, Gonzales and Mozer, 1974). As the IMF rotates northward in these models, reconnection either ceases or continues along a line passing through the subsolar point whose orientation lies close to the (northward) direction of the magnetospheric magnetic field. If

one no longer requires that the components of the magnetosheath and magnetospheric magnetic fields perpendicular to the merging line are equal in magnitude and exactly anti-parallel, merging can occur for the full range of shear angles and the subsolar merging line can assume a wide range of orientations (Cowley, 1976). In some models, patchy reconnection continues at numerous dayside locations even during intervals of northward IMF orientation (Nishida, 1989). Finally, during periods of very strongly northward IMF orientation, magnetosheath magnetic field lines may reconnect poleward of both cusps nearly simultaneously and be appended to the magnetosphere as closed LLBL magnetic field lines in the LLBL (Reiff, 1984; Song and Russell, 1992). Otherwise, reconnection takes place poleward of only one cusp, and open LLBL field lines are appended to the magnetosphere (Fuselier, 1995; Fuselier *et al*., 1997b).

Elementary comparisons of the total electric potential drops across the entire dayside magnetopause and the entire polar cap led Cowley (1982) to suggest that reconnection occurs essentially continuously in a subsolar band ~ 2 hours wide in local time, although at times its signatures have been observed on almost all portions of the magnetopause. While some ground observations during periods of strongly positive IMF B_y have been interpreted as evidence for near simultaneous reconnection over many hours of local time extending far from local noon (*cf. e.g.*, Lockwood *et al*., 1990), there are many reasons why it is difficult to imagine the simultaneous onset of reconnection over a wide range of local times (Newell and Sibeck, 1993). Instead, it is much simpler to understand reconnection that occurs in spatially localised patches and produces bundles of interconnected magnetic field lines. If the patches are very localised, the bundles may resemble the flux ropes originally drawn by Russell and Elphic (1978). With greater extent, they may resemble the short tubes illustrated by Lockwood *et al*. (1995). If reconnection is to account for the bulk of the solar wind-magnetosphere interaction, the sum of the extents of each patch must still total the observed cross-polar potential drops.

Reconnection locations inferred from *in situ* observations are quite varied, as already discussed in previous sections, ranging from subsolar to high latitude. Those observations have also demonstrated that the magnetopause can be locally closed even though the magnetic shear is high (Papamastorakis *et al.*, 1984). The likely implication is that reconnection occurs in different modes at different times, ranging from large scale and quasi-stationary to patchy and transient.

In situ measurements have shown that the magnetic field always takes the shorter path when it rotates across the magnetopause from the interplanetary to the magnetospheric direction (Berchem and Russell, 1982b). For a given direction of the IMF, the magnetopause surface can thus be divided into four regions, according to the two different signs of the normal component B_n, and the two possible senses of rotation (clockwise and counter-clockwise). These four topologically different regions are separated by singular lines, *tangential singularity* lines (TSL)

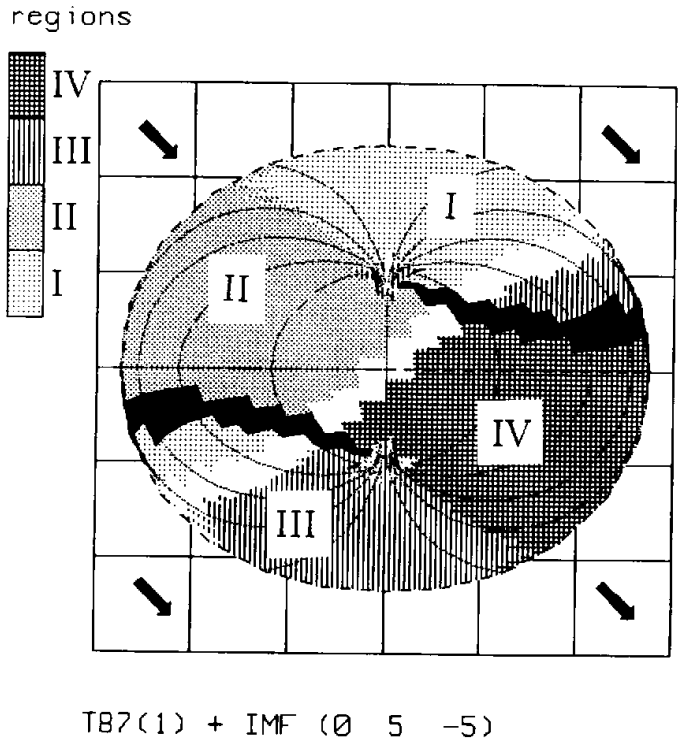

Figure 5.10. Sectorised magnetopause surface induced by an IMF (arrows) directed at an angle of 135° with respect to the z axis. Black: tangential singularities of $B_n = 0$. Different shading and numbers show the four topologically different possible sectors I-IV (figure provided by K. Stasiewicz).

where $B_n = 0$, and the *rotational singularity* lines (RSL) where the rotation changes from clockwise to anti-clockwise (Stasiewicz, 1989; 1991). The RSLs are equivalent to anti-parallel merging lines (Crooker, 1985). Figure 5.10 gives an example of a sectorised magnetopause surface in the Tsyganenko model for an IMF direction of 135°, assuming that merging occurs over the entire surface. The presence of RSLs with strongly reduced magnetic field intensity is supported by recent 3D MHD simulations (Siscoe *et al.*, 1998), but is still awaiting experimental confirmation.

Temporal Considerations

Reconnection may occur steadily. However, it seems more likely that the site and rate of reconnection constantly vary in response to changing solar wind/magnetosheath conditions and/or intrinsic magnetopause instabilities. If so, temporal considerations must be very important in determining the quantity of plasma

transferred into and out of the magnetosphere, as well as the locations where the transfer occurs.

Steady reconnection produces layers of intermingled magnetospheric and magnetosheath plasma lying on both sides of the magnetopause. The width of these layers increases with distance from the reconnection site (*e.g.*, Figure 5.4). Qualitative considerations suggest that bursty reconnection at a patch produces a small bundle of interconnected magnetosheath and magnetospheric magnetic field lines (Russell and Elphic, 1978). A single X-line produces an extended bulge of interconnected fields (Scholer, 1988; Southwood *et al.*, 1988), and the onset of simultaneous reconnection along parallel X-lines produces an extended and twisted flux rope of interconnected magnetosheath and magnetospheric magnetic field lines (Fu and Lee, 1985).

Numerical simulations provide further information concerning the phenomena that occur in response to changing reconnection rates. The results of 2-D simulations for the onset of reconnection along extended single and multiple X-lines, with and without a background magnetosheath flow, are currently available (Scholer, 1988; Ding *et al.*, 1991; Ku and Sibeck, 1997, 1998a). Simulation results for either the onset of, or bursty, reconnection at a true patch have not yet been fully explored (Otto, 1990, 1991). The newly reconnected magnetic field lines leave the reconnection site at high velocities but immediately encounter slowly moving plasma on un-reconnected magnetic field lines in their surroundings. In response to pressure gradient forces, the velocity of the newly merged magnetic field lines decreases, the surrounding plasma accelerates, and kinetic energy is converted to thermal energy within the bulge/flux rope. The heated plasma within the bulge/flux rope causes it to swell and disturb the surrounding magnetosheath and magnetospheric regions as they move along the magnetopause.

As the bulges produced by the onset of reconnection along a single reconnection line pass a spacecraft initially located in the magnetosheath, they produce strongly asymmetric bipolar magnetic field and plasma flows normal to the nominal magnetopause. Although such signatures have been observed on occasion (Rijnbeek *et al.*, 1984; Sanny *et al.*, 1998), they are not the symmetric bipolar signatures normally associated with standard FTEs (Russell and Elphic, 1978). Given the lack of success in matching signatures of bursty reconnection along an extended single reconnection line with observations, it seems likely that most observed events are produced by reconnection at patches or along multiple X-lines.

Motion of Newly Reconnected Field Lines

Newly reconnected magnetic flux tubes move over the magnetopause under the action of the pressure-gradient and magnetic curvature forces. (Crooker, 1979; Cowley and Owen, 1989). To a close approximation, the pressure-gradient force that drives the magnetosheath flow is that of the gas dynamic model (Spreiter *et*

al., 1966), regardless of the IMF orientation or strength. By contrast, the magnetic tension force depends strongly on the IMF orientation. As a result, some of the clearest macroscale predictions made by the reconnection model are those which depend upon the IMF orientation.

The magnetic curvature force that arises from reconnection is responsible for a dawn-dusk asymmetry throughout the magnetosphere which depends upon the east-west component of the IMF (B_y). In the presence of a positive IMF B_y, magnetic curvature forces at the magnetopause pull flux tubes north of the reconnection site dawnward and those south of the reconnection site duskward. The forces reverse for negative B_y. These effects of IMF B_y have been observed in subsolar flows where magnetic curvature forces can exceed the pressure-gradient forces (*cf. e.g.*, Gosling *et al*., 1990a) and at the footprints of these field lines in the ionosphere (*e.g.*, Heppner and Maynard, 1987). The curvature forces also should determine the ultimate downstream destination where reconnected magnetic field lines are deposited in the magnetotail. Spacecraft observations indeed reveal that the location of the plasma mantle depends strongly on the east-west orientation of the IMF, precisely as predicted (Hardy *et al*., 1976; Gosling *et al*., 1985).

During periods of strongly northward IMF orientation, reconnection is expected to shift to locations tailward of the cusps, and the magnetic curvature force may have a substantial sunward component directed opposite the magnetosheath flow. This sunward tension force can cause the sunward motion of plasma and field lines at the high-latitude magnetopause (Gosling *et al*., 1991; Kessel *et al*., 1996) and at its footprints in the ionosphere (Maezawa, 1976). Under these conditions, the latitudinal signatures for precipitating magnetosheath particles reverse from those discussed previously for a southward IMF. Now the cut-off dispersion is such that the most energetic particles reach the ionosphere on the poleward edge of the cusp and the less energetic particles are found at lower latitudes (Woch and Lundin, 1992a, b). Furthermore, the ions detected at the high-latitude edge of the magnetosheath precipitation appear to have experienced acceleration in the magnetopause current layer consistent with that predicted in the kinetic effects section above.

When reconnection has been occurring for some time on the dayside magnetopause during southward IMF conditions, the region of open magnetic field lines is expected to extend from the dayside reconnection site over the full downtail extent of the magnetotail. All along the area of open magnetic field lines, plasma will be able to enter the magnetosphere, with a velocity normal to the magnetopause proportional to the normal component of the magnetic field. There is strong observational evidence that this indeed happens. For example, the thickness of the plasma mantle depends strongly on the IMF B_z (Sckopke *et al.*, 1976). Furthermore, there is no gap between the magnetopause and the outer boundary of the plasma mantle (Sckopke and Paschmann, 1978; Gosling et al, 1985). Such a gap would develop as a result of the inward convection of the magnetic field

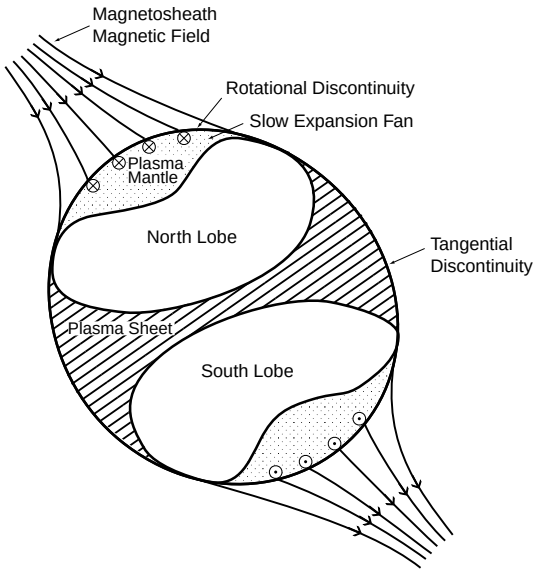

Figure 5.11. A sketch of the magnetotail cross section as seen from Earth, showing the magnetopause as a rotational discontinuity and the plasma mantle as a slow-mode expansion fan. The north-south and dawn-dusk asymmetries of the plasma mantle, as well as the tilted plasma sheet orientation are induced by a positive B_y component of the IMF (after Siscoe and Sanchez, 1987).

lines if entry were restricted to the region in the vicinity of the cusp. Note that the magnetopause in this picture is a rotational discontinuity that maintains its distance from the centre of the tail because it is standing in the flow, *i.e.* propagates upstream as fast as it advects downstream. A model for the open magnetotail boundary has been constructed by Siscoe and Sanchez (1987). Figure 5.11 shows a cross section of the magnetotail implied by this model.

The region of open magnetic field lines maps to a large area in the low-altitude polar cap, stretching from the footprint of the dayside reconnection site to the high-latitude edge of the nightside plasma sheet. The size of the open field region varies with the rate of reconnection and length of the dayside and nightside reconnection lines. Reconnection at the equatorial magnetopause increases the amount of open flux, reconnection on the polar magnetopause may diminish or leave unchanged the amount of open flux (*cf. e.g.*, Reiff, 1984).

5.2.6. GLOBAL FLUX ESTIMATES

Source Rates

Noting that there is strong evidence that reconnection often occurs in a transient and patchy manner, it is clear that isolated *in situ* measurements are inadequate to assess the solar wind plasma transfer rate across the magnetopause. In this situation one needs a more global measure, for which the cross-tail (or equivalently

the cross polar cap) electric potential seems particularly suitable, because it is determined by the amount of interconnected flux that is transported into the magnetotail each second, and estimates of the potential are available from low-altitude polar satellites.

For a completely closed magnetosphere, and disregarding magnetic field effects on the flow, only those solar wind stream lines in an infinitely narrow tube centred around the stagnation stream line come into contact with the magnetopause. When dayside reconnection occurs, however, stream lines within a finite extent, w, along the solar wind electric field, $\mathbf{E}_{sw} = -\mathbf{V}_{sw} \times \mathbf{B}$, come into contact with the magnetopause. For a purely southward IMF, w is directed along Y. When mapped onto the magnetopause by the flow, w becomes the length of the X-line. All magnetic field lines within this finite region reconnect and set up the cross-tail (or polar cap) potential, Φ_{PC}. Then by definition, $\Phi_{PC} = E_{sw}w$. Knowledge of E_{sw} and Φ_{PC} therefore determines w.

The other dimension of the cross-section of the tube of flow lines that will enter the magnetopause is more difficult to estimate. But remembering that, even when reconnection is occurring, the normal magnetic field and mass flux are both small compared with their tangential components (*cf.* Section 5.2), it seems appropriate to think of reconnection as a small perturbation on axisymmetric flow around an impenetrable object. In that case the tube cross section should be roughly circular. The flux entering the magnetosphere, F, would then be given by the solar wind flux density integrated over an area $\pi(w/2)^2$. In other words, F should scale as Φ_{PC}^2.

For typical solar wind conditions (wind speed $\sim 400\,\mathrm{km\,s^{-1}}$, density $\sim 5\,\mathrm{cm^{-3}}$, transverse magnetic field $\sim 5\,\mathrm{nT}$), the solar wind electric field is $\approx 2\,\mathrm{mV\,m^{-1}}$ and the particle flux density is $\approx 2 \times 10^8\,\mathrm{cm^{-2}\,s^{-1}}$. Typical cross-tail potentials for periods of southward IMF are 50 kV. These numbers imply $w \approx 4\,\mathrm{R_E}$ and $F \approx 3 \times 10^{27}\,\mathrm{s^{-1}}$. The $3 \times 10^{27}\,\mathrm{s^{-1}}$ must be compared with $\approx 10^{29}\,\mathrm{s^{-1}}$ that are incident on the entire magnetosphere, assuming a diameter of $40\,\mathrm{R_E}$. In other words, $\sim 3\%$ of the incident solar wind flux would enter the magnetosphere under the assumed circumstances. For the same upstream parameters, but a polar cap potential of 100 kV, the flux entering the magnetosphere should be four times larger, $\approx 10^{28}\,\mathrm{s^{-1}}$.

The numbers just derived refer to the entire magnetopause surface. Empirical estimates for the dayside magnetopause alone have given numbers of order 10^{26}. Thus only a small fraction of the total solar wind flux entering the magnetopause appears to enter on the dayside. This is not surprising, since the area of the dayside magnetopause to which the solar wind flux can gain access is much smaller than the surface extent of the magnetotail magnetopause, extending from the terminator many hundred $\mathrm{R_E}$ downstream.

Ratio of Entry and Loss Rates

A crude estimate of the ratio of entry and loss rates across the magnetopause can be obtained according to the following argument (Paschmann, 1997). The tangential electric field implied by reconnection must be continuous across the magnetopause. If the magnetic fields on the two sides have anti-parallel components, as expected for reconnection along the dayside magnetopause, then the electric field will drive plasma towards the magnetopause from both sides with equal velocities if the magnetic fields have equal strengths. In this case the ratio of entry and loss rates will simply scale as the mass-density ratio across the magnetopause, which is typically of order 10. If the magnetic field is stronger on the magnetospheric side by a factor of two, as it typically is, then the ratio increases to 20. Along the tail magnetopause, where the magnetic field direction does not reverse, the normal flow velocity is continuous and the above loss mechanism does not apply.

5.2.7. RECONNECTION SUMMARY

While there is overwhelming evidence that reconnection occurs between the magnetospheric and the interplanetary magnetic fields at the magnetopause, it is less clear why this is so. There are distinct differences of opinion as to what mechanism leads to a breakdown of the frozen-flux condition of ideal MHD within some localised region, referred to as the diffusion region. Prospective agents are anomalous resistivity, electron inertia, non-gyrotropic electron distributions, and the effect of a 'complex' equation of state and/or closure for the electrons. Using the large anomalous diffusion coefficient of $10^8 \mathrm{m}^2 s^{-1}$ derived from electric wave measurements at the magnetopause, one will not be quite as pessimistic as Scudder (1997) who concluded that "resistive MHD cannot possibly give a correct structural picture of the reconnection physics at the magnetopause". Instead, the most needed improvement is a self-consistent description of anomalous scattering in a kinetic picture of reconnection. In any case, it is evident that the details of the electron behaviour are of fundamental importance in understanding the cause of magnetic reconnection in collisionless plasmas in general, and at the magnetopause in particular.

Outside the diffusion region, ideal MHD is expected to hold and thus forms the basis of many of the theoretical predictions and their experimental tests. In this chapter, predictions and tests were subdivided into micro-, meso-, and macroscale. Microscale predictions and tests pertain to the local magnetopause and are based on ideal MHD and kinetic/multi-fluid models across one-dimensional, time-stationary rotational discontinuities. Given these highly restrictive conditions for the microscale tests, it is surprising how frequently they have been successful. The fact that on the order of $\sim 50\%$ of the cases with large magnetic shear failed to pass the tests, could imply that the magnetopause at the time and location of the

crossing was actually closed, or that the magnetopause strongly deviated from being one-dimensional and time-stationary. The (few) reported crossings which provide no trace of a boundary layer (Papamastorakis *et al*., 1984, Eastman *et al*., 1996) confirm that the magnetopause can indeed be locally closed.

It must be stressed that successful tests of tangential stress balance across the magnetopause, although implying that reconnection is or has been occurring upstream of the point of observation, do not set a value for the reconnection rate. Tests which result in quantification of the mass transfer process are difficult to perform. But even if they are successful, they only apply locally.

Microscale theory can be extended to make mesoscale predictions. In MHD, several discontinuities are required to accomplish the full transition of plasma and field parameters across the magnetopause, but only one of them has been routinely identified. In kinetic theory, consideration of velocity filter effects and an ionospheric mirror leads to numerous predictions for plasma distributions at low latitudes near the magnetopause and at high latitudes in the cusp. Information concerning the ratio of spacecraft to convection velocities is also essential in predicting the nature of the ion dispersion pattern. With relatively few free parameters, it becomes possible to predict a wide variety of ion dispersion patterns that agree well with observations.

The macroscale aspects of reconnection pertain primarily to the spatial and temporal dependence of reconnection on solar wind conditions and to estimates of the total particle transfer rates. The observations provide strong evidence for a transient and/or patchy nature of magnetopause reconnection. The evidence for reconnection on the dayside for southward IMF is overwhelming, while the evidence for reconnection poleward of the cusps at times of northward IMF is less well established. Crude estimates of the overall solar wind entry rate across the magnetopause for southward IMF, based on observed cross-tail potential drops, give numbers of order $\sim 10^{28}$ particles per second, of which only a small fraction ($\sim 10^{26}$) enters on the dayside.

In closing, it should be noted that the relationship between macro- and microscales is controversial (*e.g.*, Vasyliunas, 1988). One view holds that the micro-processes effectively adjust themselves to the macroscopic boundary conditions (*e.g.*, Axford, 1984), while another view maintains that the micro-processes affect the large scales (*e.g.*, Drake, 1984).

5.3. Finite Larmor Radius Effects

The Larmor radii of the more energetic magnetosheath and magnetospheric particles are comparable to, or greater than, the thickness of the magnetopause current layer or other boundaries in its vicinity. In Section 5.3.1 the effects of finite Larmor radii (FLR) are incorporated within the standard MHD equations. It is

then argued (Section 5.3.2) that FLR effects may contribute to the 'erosion' (inward motion) of the dayside magnetopause. The possible effects of small-scale filaments at the magnetopause are discussed in Section 5.3.3.

Energetic particles experience gradient- and curvature-drifts. They can be treated as test particles placed into a magnetopause configuration determined by the colder plasma and MHD relations. The consequences of these drifts for particle entry and exit are discussed in Sections 5.3.4 and 5.3.5, respectively.

5.3.1. FLR AND GYRO-VISCOSITY

FLR effects can modify the stress tensor in the fluid approximation by generating non-dissipative gyro-viscosities. Hau and Sonnerup (1991) have constructed one-dimensional steady state equilibrium solutions for rotational discontinuities based on a two-fluid gyro-viscous model. Those solutions exhibit significant departures from the ideal-MHD Walén relation discussed in Section 5.2.3.

Stasiewicz (1994) recently discussed FLR effects in the magnetosphere. The parameter that determines the significance of these effects is $\epsilon = r_c/L$, where r_c is the Larmor radius and L is the spatial gradient scale for plasma/field inhomogeneities. The Larmor radius of a charged particle with mass m, charge q, and velocity $v_\perp$ perpendicular to the magnetic field $\mathbf{B}$ is given by $r_c = v_\perp/\omega_c$, where $\omega_c = qB/m$ is the cyclotron frequency. In an ensemble of particles with different energies, the velocity $v_\perp$ is replaced by the mean thermal velocity $v_{s\mathrm{th}} = (k_B T_s/m_s)^{1/2}$ that determines a thermal gyroradius $r_{cs\mathrm{th}} = v_{s\mathrm{th}}/\omega_{cs}$ of a particle species $s = (e, i)$. The macroscopic velocity of guiding centres $\mathbf{u} = \mathbf{u}_\perp + \mathbf{u}_{||}$ can be also associated with a 'directed' Larmor radius $r_u = u/\omega_c$. Consequently, one can define two Larmor parameters

$$\epsilon_s = r_{cs\mathrm{th}}/L \qquad and \qquad \epsilon_u = r_u/L \tag{5.9}$$

that serve as measures of plasma and magnetic field inhomogeneities over the Larmor radius. In cases where the particle gyroradius (either thermal or directed) is comparable to the field gradient scale or to the size of plasma structures, $\epsilon \sim 1$, one often speaks about large Larmor radius (LLR) effects. For time-dependent phenomena in which $\partial f/\partial t \sim \omega f$, we have $\omega/\omega_c \sim r_c/L$, indicating that the FLR effects become increasingly important for time scales on the order of, or less than, the gyroperiod.

FLR effects enter the fluid equations through the pressure tensor in the momentum equation

$$\rho \frac{\mathrm{d}\mathbf{u}}{\mathrm{d}t} = \mathbf{j} \times \mathbf{B} - \nabla \cdot (\mathsf{P}_e + \mathsf{P}_i) \tag{5.10}$$

and through the generalised Ohm's law, which was already used in the previous section (*cf.* Equation 5.1), but is written here in the guiding centre system and for the case $\eta = 0$:

$$\mathbf{E} + \mathbf{u} \times \mathbf{B} = \frac{1}{en}(\mathbf{j} \times \mathbf{B} - \nabla \cdot \mathsf{P}_e) + \lambda_e^2 \mu_0 \frac{\partial \mathbf{j}}{\partial t} \tag{5.11}$$

where $\lambda_e = c/\omega_{pe}$ in Equation (5.11) is the electron inertial length. The first and second terms on the right-hand side of Equation (5.11) represent two-fluid, FLR effects, linear with respect to ϵ_u and ϵ_s, respectively. The third inertial term is of higher order. It becomes important in cold plasmas, $\beta < m_e/m_i$, when the inertial electron length becomes larger than the ion gyroradius, $\lambda_e > r_{ci}$.

Another class of FLR effects is related to the pressure tensor in Equation (5.10). A general expression for the pressure tensor of a collisionless plasma is

$$P_{ij} = p_\perp(\delta_{ij} - b_i b_j) + p_\parallel b_i b_j + G_{ij} \tag{5.12}$$

where $p_\parallel,\ p_\perp$ are zeroth order scalar pressure components and $b_i = B_i/|\mathbf{B}|$, with $(i = x, y, z)$, are components of the unit vector in the direction of the magnetic field $\mathbf{B}$.

The additional (FLR) terms G_{ij} represent viscosity that is independent of any collisions, produced by nonuniform flow of a collisionless plasma with finite ion Larmor radius (Kaufman, 1960; Tompson, 1961; Macmahon, 1965).

In a reference system in which the magnetic field is in the z direction the gyro-viscous tensor is

$$\begin{aligned}
G_{xx} &= -G_{yy} = -\nu\rho\left(\frac{\partial u_x}{\partial y} + \frac{\partial u_y}{\partial x}\right), \qquad G_{zz} = 0 \\
G_{xy} &= G_{yx} = \nu\rho\left(\frac{\partial u_x}{\partial x} - \frac{\partial u_y}{\partial y}\right) \\
G_{zx} &= G_{xz} = -2\nu\rho\left(\frac{\partial u_y}{\partial z} + \frac{\partial u_z}{\partial y}\right) \\
G_{yz} &= G_{zy} = 2\nu\rho\left(\frac{\partial u_x}{\partial z} + \frac{\partial u_z}{\partial x}\right)
\end{aligned} \tag{5.13}$$

The parameter ν has the dimension of a kinematic viscosity and is defined by $\nu = p_i/2\rho\omega_c$ where p_i is the perpendicular ion pressure. It can be expressed in an equivalent form $\nu = v_i^2/2\omega_{ci} = v_i r_i/2$, where $v_i = (T_i/m_i)^{1/2}$ is the ion thermal velocity and r_i is thermal gyroradius. The Reynolds number $R = uL/\nu$ is related to the gyro viscosity. For conditions encountered in the magnetopause boundary layer (Eastman *et al.*, 1985a), $T \sim 1$ keV; $u \sim v_i/2$, and $R = 2(u/v_i)(L/r_{ci}) \approx L/r_{ci}$. Since the ion Larmor radius is $\sim 100-500$ km, the Reynolds number for $L \sim 10\,\mathrm{R_E}$ is $R \sim 100-600$. Fluid dynamics with high Reynolds numbers is known to lead to turbulent flow patterns and to chaotic behaviour.

If $\nabla p \sim \epsilon_i$, then $\nabla g_{ij} \sim \epsilon_i \epsilon_u$. The gyro-viscous term in the momentum equation (5.10) represents higher order terms ($\sim \epsilon_i \epsilon_u$) than the non-ideal MHD terms in Ohm's law (5.11) that are proportional to ϵ_i or ϵ_u. Finally, for cold plasmas

$\epsilon_i \rightarrow 0$, but ϵ_u may still be large. Thus, FLR effects caused by ion inertia can occur even in cold plasmas.

5.3.2. GYRO-VISCOUS EROSION AT THE MAGNETOPAUSE

The dynamic pressure of the solar wind and the direction of the interplanetary magnetic field are the most important factors controlling the nature of the magnetopause. The location of the magnetopause is controlled primarily by the solar wind dynamic pressure p_{sw} and scales roughly as $R_s \propto p_{sw}^{-1/6}$. The magnetopause also erodes inward during periods of southward IMF, given by R_s = 11.3+0.25B_z, where R_s is expressed in Earth's radii and B_z in nT (Aubry *et al.*, 1971; Sibeck *et al.*, 1991).

The inward erosion is generally taken as evidence for reconnection and subsequent removal of magnetic flux from the dayside magnetosphere via a combination of magnetic curvature and pressure gradient forces acting upon the newly reconnected magnetic field lines (Russell *et al.*, 1974). However, it may also be possible to account for the erosion in terms of gyro-viscous stresses, which depend on the relative orientations of the magnetosheath and magnetospheric magnetic fields. With the z-axis pointing along the magnetopause normal, one obtains for the normal component of the momentum flux density tensor

$$G_{zz} + p_{\perp} + \frac{B^2}{2\mu_0} = const \tag{5.14}$$

For the tangential components one obtains

$$G_{xz} + \rho u_z u_x - \mu_0^{-1} B_x B_z = \Pi_{xz} \tag{5.15}$$

$$G_{yz} + \rho u_z u_y - \mu_0^{-1} B_y B_z = \Pi_{yz} \tag{5.16}$$

where Π_{xz} and Π_{yz} are constants, and the gyro-viscous stress is given by (Stasiewicz, 1989)

$$\begin{aligned} G_{xz} &= \nu\rho \left(b_y \frac{\partial u_z}{\partial z} + b_z \frac{\partial u_y}{\partial z} \right) \\ G_{yz} &= -\nu\rho \left(b_x \frac{\partial u_z}{\partial z} + b_z \frac{\partial u_x}{\partial z} \right) \\ G_{zz} &= -\nu\rho \left(b_x \frac{\partial u_y}{\partial z} - b_y \frac{\partial u_x}{\partial z} \right) \end{aligned} \tag{5.17}$$

The normal component of the gyro-viscous stress is equal to the field-aligned component of the tangential stress

$$b_z G_{zz} = b_x G_{xz} + b_y G_{yz} \tag{5.18}$$

so that viscous draping of the magnetic field lines along the magnetopause surface is associated with a normal stress that can change the equilibrium position of the magnetopause. The ratio of the gyro-viscous stress to Maxwell stresses is

$$\frac{\mu_0 G_{xz}}{B_x B_z} = \frac{\beta r_u}{2L} \tag{5.19}$$

where r_u is the directed ion gyroradius and L is the thickness of the magnetopause. For $\beta \sim 1-10$, as observed at the magnetopause (Paschmann *et al.*, 1986), the tangential gyro-viscous stress is comparable to the Maxwell stress. The normal gyro-viscous stress is related to field-aligned currents inside the layer via $G_{zz} = -\nu j_{\|} B_n / v_n$. Thus, the erosion is associated with field-aligned currents at the magnetopause.

It has been suggested that a normal magnetic field component, *i.e.* reconnection at the magnetopause, could be induced by gyro-viscous friction. This prediction should be verifiable using multi-point measurements such as to be provided by the Cluster mission.

5.3.3. FILAMENTARY TRANSPORT

Phenomena associated with plasma expansion into a vacuum containing a magnetic field have important applications to laboratory and space physics, and are associated with the creation of filamentary structures smaller than an ion gyroradius. Laboratory experiments with injections of plasma beams perpendicular to the magnetic field and injections parallel to a curved magnetic field may become relevant to the interaction of the solar wind with the magnetopause, if and when it is demonstrated that unmagnetised beams are present in the immediate vicinity of the dayside magnetopause.

Early experiments in which plasma was injected perpendicularly to a magnetic field of spatially increasing strength (Markovic and Scott, 1971) showed that the plasma flows until it reaches a critical value of the magnetic field strength B_c which satisfies the pressure balance relation

$$K \rho u_{\perp}^2 = \frac{B_c^2}{2\mu_0} \tag{5.20}$$

with $K \approx 2/3$. Theoretically, the coefficient K should be 1/2 for purely inelastic interaction and $K = 1$ for specular reflection of the incoming particles at the barrier. Further penetration across the magnetic barrier can occur due to the induced $\mathbf{E} \times \mathbf{B}$ drift, if polarisation charges build up at the edges of the plasma beam. A necessary condition is that the beam with velocity u_0 must have sufficient energy to create the required electric field, *i.e.* $n m_i u_0^2 \gg \epsilon_0 E^2$. With $E = u_{\perp} B$ this leads to a condition (Ishizuka and Robertson, 1982, Peter and Rostoker, 1982)

$$\omega_{pi}^2 / \omega_{ci}^2 = \epsilon - 1 \gg 1 \tag{5.21}$$

which is generally fulfilled in the magnetospheric plasma (ϵ denotes dielectric constant for the plasma). Another necessary condition results from the requirement that the maximum potential difference $e\Phi = eE_{\perp}d$ across the beam width d cannot exceed the initial kinetic energy of the beam $m_i u_0^2/2$. This condition implies that the width of a plasma structure that can dynamically generate an $\mathbf{E}\times\mathbf{B}$ drift should satisfy the inequality $d < \frac{1}{2}r_u$ where $r_u = u/\omega_{ci}$ is a gyroradius of an ion with velocity $u = u_0^2/u_{\perp}$. The above limitation was observed and first explained by Lindberg (1978). His original formula corresponds to the limit of full conversion of the beam energy into the electric drift velocity $u_{\perp} = u_0$.

The mechanism for the creation of small scale plasma structures during plasma expansion into the magnetic field is related to the Rayleigh-Taylor or interchange instability in which a heavy fluid (plasma) is decelerated by a light fluid (magnetic field). The study and observations of this instability in a magnetised plasma has largely been confined to the small Larmor radius regime $r_{ci}/L \ll 1$ and $\omega/\omega_{ci} \ll 1$, where conventional MHD theory applies.

Recent experiments performed in the FLR regime give new insight into the development of the Rayleigh-Taylor instability caused by the inertial acceleration during perpendicular plasma expansion (Huba *et al.*, 1990). When the ion Larmor radius becomes large compared to other characteristic plasma scales, *i.e.* when the ions are effectively unmagnetised but electrons remain magnetised, a related instability shows much higher growth rate than the original MHD instability. The plasma structures are smaller than an ion gyroradius and grow on times scales more rapid than the ion gyroperiod.

The plasma expansions can be categorised as being super-Alfvénic or sub-Alfvénic depending on the relative magnitude of the plasma expansion velocity to the Alfvén velocity in the background plasma. In a super-Alfvénic expansion there is a strong coupling between the expanding plasma, the ambient plasma, and the magnetic field. A shock wave is usually launched into the background plasma. In contrast to this, sub-Alfvénic plasma expansion produces much less compression and plasma interaction and, rather than launching shock waves, the expanding front launches Alfvén waves. The sub-Alfvénic expansions are notoriously unstable and usually generate plasma structures at the expanding front. The structuring process is important because it leads to significant cross-field transport via plasma jetting.

Laboratory experiments (Zakharov *et al.*, 1986; Ripin *et al.*, 1987; Okada *et al.*, 1981), as well as barium-release space experiments on HEOS (Haerendel and Lüst, 1970), with the AMPTE satellite (Bernhardt *et al.*, 1987; Hassam and Huba, 1987), and CRRES (Huba *et al.*, 1992), were all performed in the sub-Alfvénic regime. In all releases the barium plasma (1) generated a diamagnetic cavity, (2) underwent large-scale structuring, (3) expanded to a maximum size consistent with magnetic field confinement, and (4) subsequently collapsed producing an cloud elongated along the ambient magnetic field.

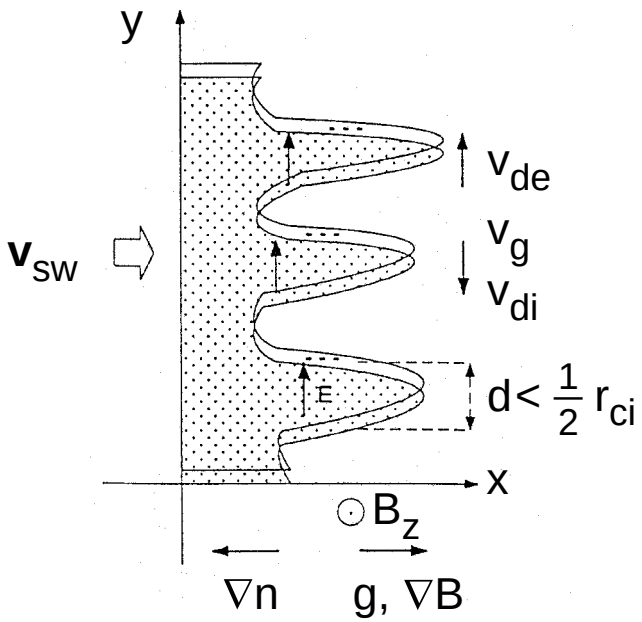

Figure 5.12. Mechanism for the plasma filamentation produced by the FLR interchange instability: An expanding plasma front breaks into small filaments that are narrower than half the gyroradius (after Ripin *et al.*, 1987).

A number of theoretical models have been advanced to explain these results. Hassam and Huba (1987) proposed an FLR Rayleigh-Taylor instability for the source of the flutes observed on the surface of the AMPTE cloud. Winske (1988) explained the same features in terms of the lower-hybrid-drift instability, which in its general form includes an electron-ion drift induced by the deceleration of the plasma across the magnetic field. The instability is driven by a deceleration of the plasma expansion front that produces a force equivalent to gravity in the reference system moving with the plasma, $g = -\mathrm{d}u_d/\mathrm{d}t$. The mechanism for the instability is related to the charge separation at a plasma front due to the differential electron and ion drifts. Both the density gradient (diamagnetic drift) and acceleration of plasma (inertial drift) contribute to the differential particle drift. Since the directed ion Larmor radius r_u is comparable to the size of the plasma cloud, this instability has been referred to as the unmagnetised ion Rayleigh-Taylor instability (Huba *et al.*, 1987) or the FLR-Rayleigh-Taylor instability (Ripin *et al.*, 1987). The mechanism for the filamentation instability is illustrated in Figure 5.12.

There have been few efforts to look for the above phenomena at the magnetopause. However, observations reported by Rezeau *et al.* (1993) and Bauer *et al.* (1998) do indicate an enhanced level of low frequency fluctuations which could represent a manifestation of the spatial structuring corresponding to plasma penetration via the FLR interchange instability.

5.3.4. GRADIENT AND POLARISATION DRIFT ENTRY

Ion composition (Lennartsson, 1992, 1997) and other plasma observations (*e.g.*, Fujimoto *et al*., 1997) have revealed that solar wind plasma gains access to Earth's plasma sheet, not only during periods of southward IMF orientation but also during times of northward IMF orientation. According to the traditional view, the magnetopause ought to be 'closed' under these circumstances. In fact, H^+ and He^{+2} ions, of apparent solar origin, reach the greatest densities (often exceeding $1\,cm^{-3}$ and $0.03\,cm^{-3}$, respectively) and the most 'solar wind-like' energies (which are of order $1-2$ keV per nucleon) during extended periods of geomagnetic quiescence, when the IMF remains strongly northward. At these times, the density of H^+ and He^{+2} ions is especially large in the dawn and dusk flanks of the plasma sheet (Lennartsson and Shelley, 1986, Fujimoto *et al*., 1997), adjacent to the LLBL (*e.g.*, Eastman *et al*., 1976, 1985b; Mitchell *et al*., 1987). Because the LLBL contains a dense plasma of solar wind origin and reaches greatest thickness during northward IMF (Mitchell *et al*., 1987), the LLBL is potentially a significant source of plasma for the plasma sheet. Once inside the LLBL, the solar wind plasma $\mathbf{E} \times \mathbf{B}$ drifts antisunward and probably into the plasma sheet and towards the tail centre (Lennartsson, 1992, 1997). The cross-tail drift may take the specific form illustrated in Figure 4 of Lennartsson (1997). The initial stage of the entry process, the mechanism by which magnetosheath plasma crosses the magnetopause, is however a more complex issue.

It is conceivable that magnetic reconnection plays an important role in supplying the LLBL with magnetosheath plasma even during times of northward IMF (*e.g.*, Fuselier *et al*., 1995), but there are nonetheless other mechanisms that may deserve more attention than they have received so far. This section is intended to revisit briefly what is arguably the least explored of all proposed interactions between solar origin particles and Earth's magnetic field, namely gradient drift entry, of magnetosheath plasma along the tail flanks (Wentworth, 1965; Fejer, 1965; Cole, 1974; Olson and Pfitzer, 1984, 1985; Treumann and Baumjohann, 1988, and references therein). The objective is not to explain this mechanism but merely to place it 'on the table' for future study. It is henceforth referred to by the acronym GDE (Olson and Pfitzer, 1984). At the end of this section, polarisation electric fields will be considered as another possible drift entry mechanism.

Olson and Pfitzer (1984) considered individual suprathermal magnetosheath particle orbits near the magnetopause to show that $1-10$ keV magnetosheath protons are deflected off the magnetopause for most directions of incidence, but that there is a narrow 'entry cone' of allowed incidence directions within 25° of the geomagnetic equator. Positive ions enter on the dawnside and electrons enter on the duskside, as illustrated in the upper panels of Figure 5.13. Particles with the opposite charges are specularly reflected. If the colder particles are treated as frozen to the magnetosheath magnetic field lines, the model predicts that the flanks of the magnetosphere would be continuously populated solely by a small

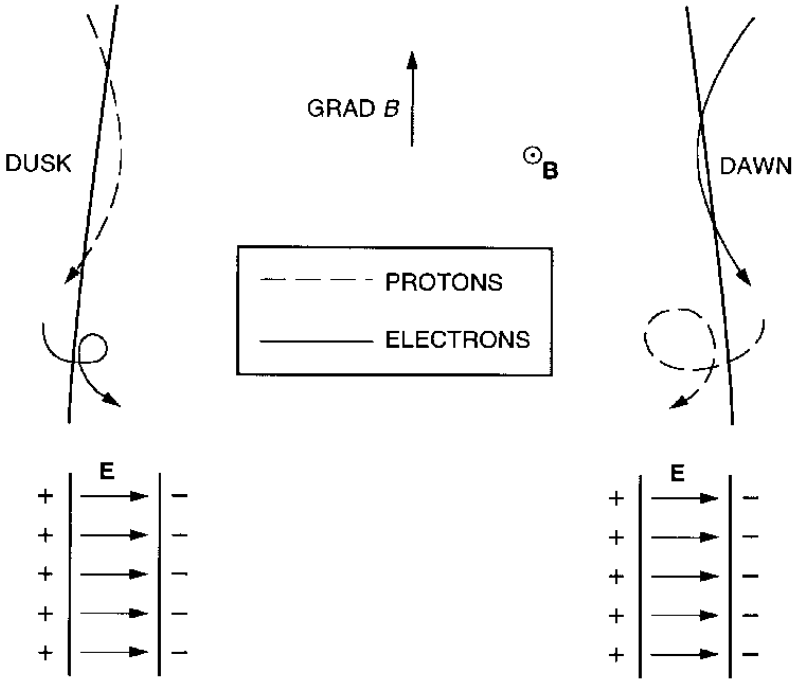

Figure 5.13. *Top*: Particle motion near the equatorial plane in a magnetotail magnetic field pointing out of the page with a gradient parallel to the magnetopause (adapted from Olson and Pfitzer, 1984; tail-flaring added). *Bottom*: Postulated boundary layer electric field.

fraction of the incident suprathermal magnetosheath plasma, primarily by protons which are substantially more energetic than the electrons. The curvature of the magnetopause may support the entry and contribute to dawn-dusk asymmetry.

Such particle drifts play an important role in the interaction of laboratory plasma beams with terrella dipole magnets, at least for protons. Cladis *et al*. (1964) considered the entry of an ionised hydrogen beam into the 'west' side of a magnetic dipole cavity. However, scaling laws suggest that such laboratory results would be more applicable to a beam of solar cosmic rays than solar wind particles.

Olson and Pfitzer (1985) proceeded to argue that all of the magnetosheath plasma striking the equatorial magnetopause directly enters the magnetosphere, thereby providing more than enough plasma to account for the observed flow of plasma down the magnetotail. However, Treumann and Baumjohann (1988) showed that no more than about 5% of the *energetic* magnetosheath plasma component may enter the LLBL by gradient drift. The main effect of this drift is to generate normal currents which locally distort the magnetopause.

The fundamental unresolved issue raised by application of a single-particle approach in the magnetospheric context is the disposal of electric charges that are

generated when protons and electrons diverge. As argued by Olson and Pfitzer (1985), charges may be redistributed via large-scale currents. They proposed that the entering particles continue to drift across the magnetotail plasma sheet, producing a current consistent with that observed. They argued that the build up of opposite charges just outside the magnetopause (due to the missing particles which have entered the magnetotail) induces a dusk-to-dawn return current across the high latitude magnetopause. Finally, they suggested that some built up charge is released as currents which flow down into the ionosphere in the observed region-1 Birkeland current sense.

If not stopped, the entering particles would simply gradient-curvature drift across the magnetotail, gaining energy from the normally dawn-to-dusk electric field within the plasma sheet. This would result in a distinct dawn-dusk asymmetry in H^+ and He^{+2} ion energies, which conflicts with observations indicating peak energies near the tail centre (Lennartsson and Shelley, 1986). Another possibility is that a polarisation electric field develops in the boundary layer, as indicated in the bottom part of Figure 5.13, which forces the plasma to drift antisunward. The thickness of the LLBL is not related in a simple manner to either the inward drift speed or the particle gyroradii, because the sunward gradient in the tail magnetic field is associated with a flaring of the magnetopause, which implies that different magnetosheath particles can enter at different distances from the tail axis.

To date, the self-consistent effects of the induced electric field in such a boundary layer have not been considered. Pure gradient-B drift must progress at a rather modest speed near the dawn and dusk magnetopause, on the order of ~ 0.1 km per minute per eV of particle energy (Treumann and Baumjohann, 1988). Charge separation effects become significant on Debye length spatial scales, on the order of tens of metres in this region of space (where electron densities are several cm^{-3} or more, and thermal energies are at most a few hundred eV), which is small even compared to electron gyroradii (which are $\sim$ 2 km in a 20 nT field for particles with energies of 100 eV). Hence, pure ∇B-drift is virtually impossible and interparticle electric forces must become significant within a single gyration of the entering particles, be they protons or electrons.

Two major predictions emerge if entry were to occur solely by the gradient-drift mechanism. Gradient-drift entry predicts (1), a steady antisunward flowing plasma in the boundary layer, regardless of IMF orientation, and (2), an increase in the total flux of plasma flowing tailward on closed magnetospheric magnetic field lines with downstream distance. However, the available tail observations do not necessarily confirm the presence of a dense region of antisunward flowing plasma on closed magnetic field lines. While the plasma sheet velocity definitely increases with downstream distance (Zwickl *et al.*, 1984; Paterson and Frank, 1994), the density may (Zwickl *et al.*, 1984) or may not (Paterson and Frank, 1994). The increase, if any, in antisunward flux is generally considered to occur on southward, or open, magnetic field lines produced by reconnection in the mag-

netotail plasma sheet (Slavin *et al*., 1985). Whether the contribution from gradient drift is significant remains to be seen. It may be necessary to use hybrid or particle simulations in order to account for gradient drift and space charge effects.

By comparison with gradient-drift entry, another potential drift entry mechanism, caused by electric polarisation, has received even less attention. The difference in the electron and ion gyroradii may cause a charge separation electric field at the magnetopause (see bottom of Figure 5.13). Temporal variations of this polarisation field will generate polarisation drifts of the ions normal to the magnetopause. If one postulates that this field varies on the time scale of the ion gyro frequency, with an amplitude of a few $\mathrm{mV\,m^{-1}}$, an ion drift of order of a few $\mathrm{km\,s^{-1}}$ would result. Such drifts would be significant for particle entry.

5.3.5. GRADIENT DRIFT EXIT

Thermal and energetic particles of magnetospheric origin are commonly observed within a narrow magnetosheath layer at and immediately outside all regions of the magnetopause (Meng and Anderson, 1970; Hones *et al*., 1972). The extrapolated energy flux carried by electrons with energies in excess of 10 keV ranges from 3×10^8 during quiet times to 3×10^{11} W during disturbed times (Baker and Stone, 1977). Ions with energies in excess of 50 keV carry a similar energy flux (Williams, 1979). We know that these particles are of magnetospheric origin because their composition (Sonnerup *et al*., 1981; Peterson *et al*., 1982) and spectra (Williams *et al*., 1979) are similar to those for particles immediately inside the magnetosphere. The flux of energetic electrons is greatest outside the dawnside magnetopause, and the flux of energetic ions is greatest outside the duskside magnetopause (Meng *et al*., 1981), consistent with the fact that the ions gradient and curvature drift westward, and the electrons eastward, to the points where their drift paths intersect the magnetopause. Spacecraft immediately inside the magnetopause can remotely sense a loss boundary from which ions do not return (Williams *et al*., 1979). Moreover, the loss of electrons with 90° pitch angles from the pre-noon magnetopause is manifested by their absence from so-called 'butterfly' pitch angle distributions in the post-noon magnetosphere (West *et al*., 1973). Similarly, the loss of ions from the post-noon magnetopause is manifested by their absence from butterfly pitch angle distributions in the pre-noon magnetosphere (Sibeck *et al*., 1987c). Finally, flux levels in the magnetosheath increase with increasing geomagnetic activity (Frank and Van Allen, 1964; Meng and Anderson, 1970, 1975; West and Buck, 1976), consistent with the fact that flux levels within the magnetosphere itself increase with increasing activity.

While the above observations provide overwhelming evidence that the magnetosphere generally provides the main contribution to the energetic particle population found within the inner magnetosheath, the question of how the magnetospheric particles escape remains open. They are free to stream outward along

interconnected magnetosheath and magnetospheric magnetic field lines (Speiser *et al*, 1981) and observations of their anisotropies parallel or opposite to magnetosheath magnetic field orientations have often been taken as evidence for the presence of the tilted subsolar reconnection predicted by some models (*cf. e.g.*, Daly *et al*., 1984).

Magnetic reconnection is not the only means by which magnetospheric particles may escape from the magnetosphere into the magnetosheath (*cf. e.g.*, Sibeck and McEntire, 1988). Energetic magnetospheric ions with energies of ~ 100 keV (and the very rare energetic electrons with energies of ~ 200 MeV) have gyroradii comparable to the ~ 800 km median thickness of the magnetopause current layer reported by Berchem and Russell (1982a). The orbits of particles with energies of this order simply pass across the magnetopause. With or without the presence of a finite magnetic field component normal to the magnetopause, the particles will be scattered in the current layer. Some precipitate into the ionosphere (Lyons *et al*., 1987), but most probably stream away from the magnetosphere into the magnetosheath. In fact, the very same anisotropy observations used to confirm that ions escape from the magnetosphere along reconnected field lines are entirely consistent with escape via gradient-curvature drift (Sibeck *et al.* 1987b). The fact that the energetic ions are present outside the magnetopause for both northward and southward IMF conditions suggests that they are always escaping whether or not conditions favour reconnection (Sibeck *et al*., 1987a,b).

5.4. Diffusion

5.4.1. INTRODUCTION

The focus of this section is on cross-field diffusive plasma entry and exit processes as possible mechanisms for cross-magnetopause plasma transfer. This includes micro, macro, and turbulent diffusion processes. Cross-field diffusion of cool sheath plasma into the LLBL may play a significant role in regions where or under conditions when magnetic reconnection is not operative or is not efficient. Such conditions may in particular be realised when the sheath magnetic field, which is the compressed interplanetary magnetic field, points northward.

The role of diffusion can, in principle, be deduced by observing the flow and field characteristics of the LLBL, together with the magnetic topology of the region, for example, from the observed spatial profiles of the LLBL. Sharp changes in the profiles may correspond to boundaries or discontinuities associated with reconnection (*cf. e.g.*, Gosling *et al*., 1990; Song *et al*., 1994). Smooth and gradual profiles may be indicative of diffusive plasma entry (*cf. e.g.*, Thorne and Tsurutani, 1991). The variation of the thickness of the LLBL along the magnetopause with increasing distance from the subsolar point also contains information on the magnetopause processes. A lack of increase of the thickness would be

inconsistent with continuous diffusive plasma entry, whereas a widening of the LLBL on closed field lines would indicate efficient diffusive transport. However, one could envision that reconnection can produce a boundary layer on closed field lines as well when the reconnection takes place at two locations along the same flux tube (*cf. e.g.*, Song and Russell, 1992). Otherwise, an LLBL on open field lines is clearly indicative of reconnection. Thus, in order to distinguish diffusion from reconnection, one needs to compare the theoretical predictions with detailed examinations of the particles and fields. A detailed account of the diffusion processes in provided in Appendix B.

5.4.2. DIFFUSION PROCESSES

The treatment of diffusion processes is based on the assumption of stationarity of the diffusive flows. The diffusive velocity is determined by the diffusion tensor D, whose components are the diffusivities parallel and perpendicular to the magnetic field: $\mathsf{D} = (D_\perp, D_\perp, D_{||})$. The diffusivity is defined as $D = v_{th}^2/\nu$, the ratio of the square of the thermal velocity v_{th} and the (usually anomalous) collision frequency ν.

Diffusion makes sense only in an inhomogeneous plasma and is thus limited to the various boundaries in the magnetosphere. Diffusion naturally requires a distortion of particle orbits in the presence of some kind of particle scattering. In the fluid picture it implies a violation of the frozen-in concept for the fluid element. Scattering implies that some irreversible mechanism is acting. Formally its effect can be taken into account via a (real or anomalous) collision frequency ν. The component of D parallel to the external magnetic field $\mathbf{B}$ is then given by $D = D_{||} = k_B T/m\nu$ for each particle component, ions and electrons (i, e). Imposing quasi-neutrality yields the ambipolar diffusivity $D_a = (\mu_e D_i + \mu_i D_e)/(\mu_i + \mu_e)$. Here $\mu = |q|/m\nu$ is the mobility of particles of mass m and charge q. The ambipolar diffusion coefficient of the plasma perpendicular to the magnetic field is given by

$$D_\perp = r_{ce}^2 \nu (1 + T_{\perp i}/T_{\perp e}) \tag{5.22}$$

where $r_{ce} = v_e/\omega_{ce}$ is the (thermal) electron gyro-radius. Because the electron and ion gyro-radii are so different, ambipolarity is a very involved concept. From these expressions it becomes clear that in the absence of collisions, $\nu = 0$, there is no diffusion even in an inhomogeneous plasma. Thus diffusion depends essentially on the presence of a mechanism that provides sufficiently strong particle scattering. In the absence of actual particle collisions, such mechanisms can be provided by wave particle interactions. The most important of them are discussed in Appendix B. To distinguish them from ordinary collisional diffusion one speaks of *anomalous resistive* diffusion.

Because the magnetopause is a transverse current layer, accompanied by density, temperature, magnetic field, and flow gradients, there are a large number

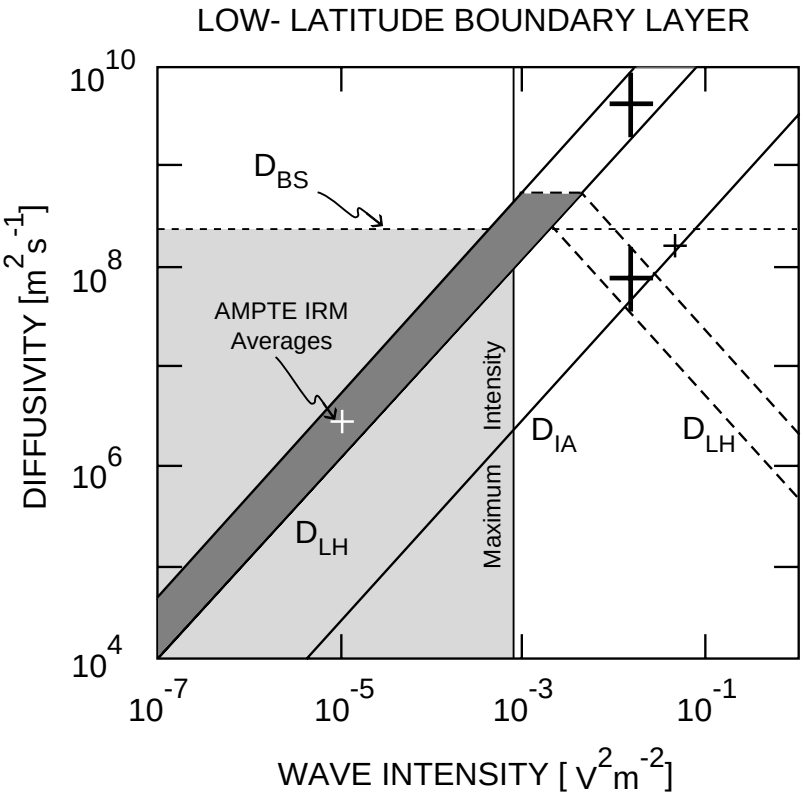

Figure 5.14. Estimated diffusivities for the ion-acoustic (D_{IA}) and lower-hybrid (D_{LH}) drift instabilities using electrostatic wave measurements in the LLBL. D_{BS} is the Bohm-Sonnerup limit. The diffusivities are scaled for the inner part of the LLBL. For the lower-hybrid drift instability the range of uncertainty is given by the darkened strip. The shaded region shows the domain of spacecraft measurement of electric wave amplitudes. Crosses indicate theoretical quasi-linear estimates of saturation amplitudes adjusted to the diffusion curves. Two different diffusivity models are shown for the lower-hybrid drift instability (dashed lines). The decrease of the diffusion coefficient for extremely high powers is due to diffusion becoming isotropic. In this case $D \propto 1/\nu$ (after Treumann *et al*., 1995).

of candidate instabilities for anomalous diffusion (*cf.* Appendix B). The micro-instabilities among them may be divided into current instabilities and drift instabilities. The table in Appendix B summarises their properties. Inspection of that table shows that the most promising instability is the lower-hybrid drift instability which causes anomalous collision frequencies on the order of the lower-hybrid frequency, $\nu_{an} \approx \omega_{LH}$.

A number of macro-instabilities can also contribute to diffusion. Among them the Kelvin-Helmholtz instability and eddy turbulence may be important (*cf.* Appendix B). The former is discussed in more detail in Section 5.5. Eddy turbulence, on the other hand, is only vaguely defined and awaits further investigation. Both

instabilities may contribute by stirring the plasma over larger scales and providing the background motion for micro-instabilities which may actually scatter the particles into diffusive orbits. Convective cells (Taylor and McNamarra, 1971) as well as the magnetostatic modes (Chu *et al.*, 1978) also belong to this class of instabilities. Moreover, the effect of kinetic Alfvén modes (Hasegawa and Mima, 1978) may not be negligible (Lotko and Sonnerup, 1995).

Two further effects must be considered. The first is pitch-angle scattering in strong wave fields (Tsurutani and Thorne, 1982; Thorne and Tsurutani, 1991), which resonantly scatters particles out of their Larmor orbits. The second effect occurs in the time-dependent regime, where particles may no longer be subject to stochastic motion, but follow a different kind of statistics known as Lévy flights. If this applies than diffusion may be enhanced whenever the system evolves in time (Treumann, 1997).

5.4.3. OBSERVATIONS SUGGESTIVE OF DIFFUSION

The observational studies of diffusion have thus far concentrated mainly on three aspects: (1) measuring the electric and magnetic fluctuations within the LLBL for comparison with theoretical models; (2) inferring the magnetic topology of the LLBL and its dependence on the external IMF orientation; (3) deducing the spatial structure and the thickness of the LLBL and their relationships with the external magnetosheath conditions.

Electric Wave Intensities

The saturation levels and corresponding diffusion coefficients given in the table in Appendix B are theoretical estimates which must be verified experimentally. Experimental verification of the resistive diffusion has been attempted on the basis of measurements of the wave electric and magnetic intensities in the LLBL. Wave observations at the magnetopause have been presented by Gurnett *et al*. (1979b), Anderson *et al*. (1982), LaBelle and Treumann (1988), Tsurutani *et al*. (1989) and others. A summary of the measurements is given in Figure 5.14. In this figure the current-driven ion-acoustic and lower-hybrid drift diffusion coefficients are plotted as function of the electric wave intensity. Only these two instabilities are of practical interest because the Buneman instability will barely be realised in the LLBL. Presumably, other current driven instabilities are irrelevant as well.

Inspection of Figure 5.14 leads to a number of important conclusions. In the log-log presentation used in the figure, current driven diffusion coefficients plotted as functions of wave intensity are straight lines shifted by different amounts in the vertical direction. This shift depends on the particular nature of the instability. In order to obtain a diffusion coefficient high enough for the *inner* LLBL, on the order of $D_{\mathrm{B}S} \approx 2\times 10^{8}\,\mathrm{m^2 s^{-1}}$ (upper horizontal line in the figure), one needs lower-hybrid wave electric field amplitudes of $\delta E_{\mathrm{L}H} > 30\,\mathrm{mV\ m^{-1}}$. The ion

acoustic instability would require even higher field strengths.

Figure 5.14 shows that the highest measured wave intensities occasionally reach about $10^{-3}\,\mathrm{V^2\,m^{-2}}$ (vertical line). The shaded region shows the domain of realistic wave amplitudes. It is evident that only for the highest intensities does the lower-hybrid drift diffusion coefficient marginally reach the LLBL Bohm-Sonnerup limit. For lower wave intensities it stays relatively far below the required value, suggesting that diffusion is just marginally able to fill the inner LLBL. Ion-acoustic diffusivities are generally too low except in extraordinary cases of extremely high wave intensities. One would thus conclude that none of the electrostatic turbulent modes may, under normal conditions, build up the inner LLBL by a purely diffusive process based on resistive diffusivities.

The coincidence of the lower-hybrid diffusivity with Bohm-Sonnerup diffusion in the inner LLBL for the highest measured wave electric amplitudes is intriguing. Possibly this is only a chance coincidence, but, on the other hand, it might indicate that the inner LLBL is sporadically in diffusive equilibrium with the lower hybrid wave intensities caused by the density and temperature gradients. In such a diffusive equilibrium the diffusion would just flatten the density gradient to a self-supporting inclination, where the gradient causes the residual wave fields to keep the diffusion at the marginal Bohm-Sonnerup level.

Statistical studies of AMPTE/IRM magnetopause crossings (Bauer *et al*., 1998) showed that, for the conditions within the inner LLBL, the average electric wave amplitudes are low, in general not larger than $\delta E \approx 0.1\,\mathrm{mV\,m^{-1}}$. But the sporadically appearing amplitudes can be as high as $\delta E \approx 1\,\mathrm{mV\,m^{-1}}$ and, for northward interplanetary field, are centred at the inner edge of the LLBL. High time resolution observations of other spacecraft deeper inside the magnetosphere (FAST, Polar) suggest even higher sporadic electric wave fields on the order of $\sim 1\,\mathrm{V\,m^{-1}}$. This confirms the above conclusions that high diffusivities occur only sporadically. An empirical relationship between the low-frequency waves and the magnetic shear at the magnetopause has been established by Zhu *et al*. (1996).

On the other hand, it is reasonable to assume that even for moderate wave activity levels caused by the lower-hybrid drift instability (as well as that the ion-acoustic mode) provide enough diffusivity to ignite reconnection in the narrow localised diffusion region of reconnection. The diffusivities, nearly continuously present in the steep density and temperature gradients across all the dayside magnetopause, are high enough to ignite reconnection locally wherever the magnetic fields on both sides of the magnetopause have antiparallel components. These diffusivities are the necessary prerequisite for the onset of such patchy reconnection.

Measured electric field intensities still suffer certain deficiencies: they lack a continuous fast time resolution, determination of wave vectors, and do not allow unambiguous resolution of wave modes. There is little knowledge about the wave polarisation, effects of antenna length in regions with varying Debye radii, and

there is no determination of the spatial variations of the wave spectra, their source regions and group velocities. In addition the particle distributions are not measured quickly and precisely enough to allow for the determination of the kinetic sources of instabilities in the narrow boundary layers, not to mention the ambiguities of a single point measurement in space. These difficulties are compounded by theoretical deficiencies in determining the diffusivity on the basis of quasi-linear theory alone. Wave-wave and wave-particle interactions as well as other nonlinear processes are not included in the theory.

Topology

Particle behaviour provides indications of the LLBL topology. The particle signatures that have been taken as indicators for closed-field topology include: (1) trapped magnetospheric particle distributions (Mitchell *et al.*, 1987), (2) counter-streaming low-energy (~ 10 eV) electrons with balanced fluxes (Song *et al.*, 1993), (3) counter-streaming medium energy electrons ($50-400$ eV) and ions with balanced fluxes (Ogilvie *et al.*, 1984; Hall *et al.*, 1991; Traver *et al.*, 1991; Smith and Rodgers, 1991; Fujimoto *et al.*, 1996; Bauer *et al.*, 1997). The presence in the LLBL of unidirectional field-aligned electrons of any energy implies an open-field topology. Composition measurements (Fuselier *et al*. 1997a) suggest that the entire LLBL lies on open field lines, even when the IMF is northward.

For a northward IMF, counter-streaming electrons are observed throughout the entire LLBL (Mitchell *et al.*, 1987; Traver *et al.*, 1991; Fuselier *et al.*, 1995, 1997b; Phan *et al.*, 1997). Taking counter-streaming electrons as evidence for closed field topology, one would conclude that the entire dayside LLBL is on closed field lines when the IMF is northward. It has, however, been pointed out that a bi-directional field-aligned electron signature alone is not conclusive evidence for closed-field topology (*cf. e.g.*, Daly and Fritz, 1982; Fuselier *et al.*, 1995, 1997b). Magnetosheath electrons which cross the magnetopause and bounce back after being mirrored at lower altitudes also give rise to counter-streaming signatures. Thus, to convincingly deduce the field-line topology of the boundary layer, one would need to examine the behaviour of electrons originating from the magnetosheath, magnetosphere and ionosphere. In addition to the electron signatures, information on ions (and especially ion composition) could prove decisive for determining the topology.

Spatial Profile and LLBL Thickness

The spatial structure of the LLBL is of interest since it provides an indication as to whether or not diffusion plays a role in formation of the LLBL. For diffusive plasma entry one expects smooth and gradual density, temperature, and flow profiles, together with close coupling to the properties of the adjacent magnetosheath. Sharp gradients bordering plateau profiles, on the other hand, may be consequences of reconnection, although time-of-flight effects associated with

reconnection may also give rise to gradual profiles of density and temperature (see, *e.g.*, Lockwood and Hapgood, 1997).

Gradual, abrupt and plateau-like profiles have been found in time series of magnetopause crossings. From single spacecraft measurements it is difficult to determine whether the time series are representative of the spatial variations. There are indications that some of the time variations result from the irregular motion of the magnetopause. Average temperature variations are smooth and gradual when plotted against density variations (Hapgood and Bryant, 1990; Hall *et al*., 1991). The plasma flow velocity component tangential to the magnetopause is also well-correlated with the density (Fujimoto *et al*., 1996). Paschmann *et al*. (1990) used single spacecraft normal velocity (v_n) data to deconvolve a temporal density profile into a spatial one. For the one event that they analysed, the deconvolved profile seems gradual. However, the method depends heavily on the accuracy of the magnetopause normal determination (Paschmann, 1997). Thus, in the absence of multi-spacecraft missions, true spatial profiles remain unknown.

Flows in the magnetosheath and the LLBL are often nearly aligned, as expected for diffusive plasma entry (Eastman *et al*., 1985a; Mitchell *et al*., 1987). Phan *et al.* (1997) have confirmed this for low magnetic shear, but also found high shear cases where this was true for the inner LLBL, even though reconnection flows - which usually are not aligned with the sheath flow - were detected at the magnetopause and in the outer LLBL.

Finally, there are estimates of the LLBL thickness and its evolution with distance from the subsolar point. Mitchell *et al*. (1987) found that the LLBL thickness grows away from the subsolar point, consistent with diffusion, while Phan and Paschmann (1996) reported no such trend. Instead, they observed large variations in the LLBL thickness from case to case. Thus the question of the evolution of the LLBL remains open until better methods of measurement or analysis become available. It should, however, be noted that the behaviour of the magnetopause changes drastically from the dayside towards the flanks, where different conditions are met (Scholer and Treumann, 1997) and diffusion may be of greater importance.

5.4.4. DIFFUSION COEFFICIENT

Definition

Experimental determination of diffusivities requires a definition of diffusion coefficients independent of theory. Under the assumption that diffusion is the dominant process, the diffusion equation (*cf.* Appendix B) suggests two different definitions of the diffusion coefficient.

Let us assume that the diffusion process is one-dimensional and proceeds in the direction $\mathbf{n}$ normal to the boundary (this simplification does not generally hold but is specific to conditions where the diffusion is caused by a density ramp). It

then follows from the continuity equation and from the diffusion equation,

$$\frac{\partial n}{\partial t} = D\nabla^2 n \tag{5.23}$$

that the following relation holds between D, the density n, and the component of the flow velocity, v_n, normal to the density gradient contours:

$$D\nabla_n n = -nv_n \tag{5.24}$$

This then yields the one-dimensional definition equation for the diffusion coefficient

$$D = -\frac{v_n}{\nabla_n(\ln n)} = -\frac{v_n \Delta x}{\Delta(\ln n)} \tag{5.25}$$

Similarly, the induction equation leads to an expression of the kind

$$D_m = -\frac{v_n}{\nabla_n(\ln|\nabla_n B_T|)} = -\frac{v_n \Delta x}{\Delta[\ln|\Delta B_T/\Delta x|]} \tag{5.26}$$

where we have assumed a stationary diffusion process such that $\partial\mathbf{B}/\partial t = -\mathbf{v}\cdot\nabla\mathbf{B}$. B_T is the component tangential to the magnetopause. For practical reasons it is convenient to replace the spatial derivatives in these expressions by the local time derivatives, which gives instead

$$D = v_n^2 \frac{\Delta t}{\Delta(\ln n)} \tag{5.27}$$

and in the second case

$$D_m = v_n^2 \Delta t \left[\Delta \ln\left|\frac{1}{v_n}\frac{\Delta B_T}{\Delta t}\right|\right]^{-1} \rightarrow v_n^2 \frac{\Delta t}{\Delta \ln|\Delta B_T/\Delta t|} \tag{5.28}$$

where in the second part of the equation it is assumed that v_n varies more slowly than B_T.

These formulae can be applied to regression analysis of data in the boundary layer. The former expression is easier to treat but requires high resolution measurements of the density. In the boundary layer this is difficult to achieve with available plasma instrumentation. On the other hand, high resolution measurement of either the electron plasma frequency or the magnetospheric trapped radiation cut-off can help determine the density changes on sufficiently fast time scales.

The second expression is more difficult because of the higher order derivative of the magnetic field appearing in it. If it is assumed that the transverse speed v_n is constant, then one of the derivatives drops out and the expression simplifies. An advantage of this formula is that the magnetic field is known with rather good time resolution in the boundary layer. On the other hand, reckoning the magnetic field profile using the measured v_n will make the profile independent of time. This

also holds for expression (5.27) for the density profile. In any case both formulae depend heavily on the knowledge of the normal velocity.

Another practical form of the diffusion coefficient is (Paschmann, 1997)

$$D\frac{\Delta n}{\Delta x} = \langle nv_n\rangle - \langle n\rangle\langle v_n\rangle \tag{5.29}$$

Angular brackets imply ensemble averages over the locally measured densities and normal velocities. Uncertainties in the normal velocity will introduce ambiguities into the determination of the diffusion coefficient.

Postulated Diffusion Coefficient

Sckopke *et al*. (1981) tested whether diffusive entry was able to populate the LLBL. From a single magnetopause crossing, they found a value of $D_\perp \approx 10^9$ m^2 s^{-1} which has been widely used as a test of various candidates of diffusion mechanisms. In a number of theoretical studies of the diffusion processes, a process has been deemed not valid for the LLBL when it cannot achieve the required coefficient. Thus it is important to understand how this number was obtained and how it may vary from case to case. In what follows, first a description is given of the method and the assumptions used. It is then pointed out that although Sckopke's *et al*. (1981) estimate was crude and was based on only one event, the minimum 'required' diffusion coefficient is not expected to be substantially below 10^9 m^{2}s^{-1}.

If one takes a certain boundary layer average width w, density n, and bulk speed v, the resulting flux per unit height is $F = wnv$. At an observation point a distance L away from the subsolar point, the average flux density across the magnetopause is $\langle F\rangle = wnv/L$. If attributed entirely to diffusion, this flux should equal to $\langle F\rangle = D\delta n/h$, where D is the diffusion coefficient and δn the density change across the diffusion layer of thickness h. Note that the diffusion layer may be substantially thinner than the boundary layer itself if one envisions diffusion to occur only across the thin topological boundary (the magnetopause), and additional processes such as eddy viscosity provide further transport to populate the remaining LLBL.

For the flank (L = 18 R$_E$) crossing that Sckopke *et al*. (1981) investigated, w = 0.5 R$_E$, n = 8 cm^{-3}, δn = 27 cm^{-3}, v = 150 km s^{-1}, yielding D/h = 2.5 $\times$ 10^3 m s^{-1}. Thus the value of D depends on the thickness h of the layer across which diffusion takes place. Sckopke *et al*. (1981) assumed that diffusion occurred across the magnetopause (with a typical thickness of 400 km), resulting in $D \sim 10^9$ m^2 s^{-1}.

The diffusion coefficient is expected to vary from crossing to crossing. Taking into account the variations in w and h Phan and Paschmann (1996) obtained $w \sim 0.01-1.5$ R$_E$ in the 8–16 LT range), the expected experimental range in

which D may vary is

$$2 \times 10^7 < D < 3 \times 10^{10} \quad \mathrm{m^2 s^{-1}} \tag{5.30}$$

5.4.5. DIFFUSION SUMMARY

A number of processes have been reviewed that may cause diffusion in collisionless plasmas. It is most important to understand that diffusion is basically a resistive process which dominates only when high resistivities are generated and when any other competing processes can be neglected. We have not discussed what the combined effect of such processes would be. The dominant gradient driven instabilities are the lower-hybrid drift instability and the ion-acoustic current driven modes. Available measurements do not yield sufficient diffusion on average. However, sporadic high diffusion may be just marginal for the lower-hybrid drift instability. For much higher wave fields the diffusion coefficient from the lower-hybrid drift instability probably decreases again, and the diffusion process is taken over by the ion-acoustic mode.

There are many sources of free energy in the magnetopause region, such as gradients in density, temperature and magnetic field as well as pressure anisotropies, currents, flow shears *etc*. Therefore, one does not expect a single instability to dominate. Instead, a broad spectrum of competing instabilities will arise. The presence of this spectrum will affect the growth of those instabilities which would ordinarily contribute to diffusion the most.

Magnetic spectra seem to indicate that diffusion by magnetic fluctuations is possible. The basic mechanism is probably field line mixing (stochasticity) which is some chaotic version of the reconnection process. Other diffusion theories can be based on more exotic processes like Lévy flights. In this case diffusion is not classical but time-dependent.

For some of these processes it is very difficult to design tests simply because the process itself is not well defined and still questionable. The situation is similar to that in fusion theory and experiment where one believed that the basic processes and losses were well understood. Space plasma physics suffers from the measurements being intermittent and imprecise in space, time and energy, both for the particle distribution function and wave spectra. Improvement is expected from future multi-spacecraft missions like Cluster.

A diffusion coefficient of $D = 10^9\,\mathrm{m^2\,s^{-1}}$ has frequently been used to test the validity of diffusion for transfer of plasma across the magnetopause. It should be remembered that this number arises from consideration of a specific case. The 'required' diffusion coefficient may vary substantially from case to case due to large variations in the boundary and diffusion layer thicknesses.

While it may be doubted that diffusion is adequate to populate the low-latitude boundary layer, there can be no doubt that the estimated diffusivities are locally high enough for the onset of reconnection. The diffusivity provides the

sufficient condition for reconnection, whether it is stationary or is sporadic and localised, as in FTEs or in 'intermittent reconnection' (Chang, 1998). Reconnection opens up the simplest path for plasma to stream into the inner LLBL along the magnetic field lines. One thus expects that in combination with localised diffusion, reconnection is the dominant transport process and thus the dominant magnetopause source (and loss) process, after it has re-organised the magnetic topology somewhere on the magnetopause. Diffusion is then required only in the narrow local diffusion region. This is a very weak requirement. But the properties of the diffusion region are still under debate. The remaining questions are: Is this region highly turbulent or not? What are the relevant wave modes in this region? Are the modes magnetised or unmagnetised? Simulation and analytical studies of transport processes in collisionless plasmas including long-range correlations and improved measurements are needed before these controversial problems ultimately can be settled.

5.5. Kelvin-Helmholtz Instability

5.5.1. INTRODUCTION

The magnetopause, a thin discontinuity frequently marked by a considerable velocity shear, should be an ideal location for the Kelvin-Helmholtz instability (KHI). The other macroscopic instabilities that can develop in collisionless interacting plasmas, like the Rayleigh-Taylor, interchange, and kink instabilities, may be ignored because gravitational effects which might drive the Rayleigh-Taylor and interchange modes, as well as the strongly localised currents which cause sausage instabilities or kink instabilities, are practically absent at the radial distance of the magnetopause from Earth.

The KHI occurs in hydrodynamics as well as in magnetohydrodynamics, where the magnetic field, through its component along the shear direction, exerts a stabilising force (Southwood, 1968; Hasegawa, 1975). In the particular application of plasma transport at the magnetopause, the situation is complicated because the shear is a function of position and time and because boundary layers exist, providing a second surface which can become unstable.

If this instability develops one expects several effects: (1) The flow patterns generated will distort the smooth magnetopause surface and boundary layer on the macroscopic scale of the most unstable wavelength, which is comparable to the boundary layer thickness (Walker, 1979). (2) Large-scale flow patterns necessarily lead to momentum transport across the magnetopause and boundary layer. (3) They also include large-scale eddies which may reach relatively deeply into the magnetosphere or out into the sheath. (4) Any sharp local boundaries generated by the KHI will enable smaller scale or microscale instabilities to evolve and may thus contribute to local increases of diffusivity. (5) In this way the KHI

can contribute to plasma mixing and mass transport. (6) Mixing of the fluid also implies mixing of magnetic fields. Hence the KHI may support the local development of reconnection and could in fact contribute to the formation of FTEs (*cf.* La Belle-Hamer *et al*., 1995). This catalogue of expectations, as recognised early in magnetospheric research, shows the potential importance of the KHI for magnetopause plasma transport.

5.5.2. THEORETICAL DEVELOPMENTS

The basic linear theory has been summarised in the classical book of Chandrasekhar (1961). The presence of magnetic fields strongly affects the evolution of the KH instability. Linear analyses indicate that a magnetic field component parallel to the flow shear inhibits the growth of the KHI. For early reviews of the magnetised KHI we refer the readers to Southwood (1968) and Hasegawa (1975). These authors present models that treat sharp shear boundaries at the magnetopause and are therefore highly idealised. Fitzenreiter and Ogilvie (1995) and Scholer and Treumann (1997) report more recent theoretical achievements in KHI theory.

The properties of the Kelvin-Helmholtz instability form a suitable subject for computer simulation. Simulations can be used to investigate the dependence of instability growth rates on the magnitude of the velocity and magnetic field strength and shears. An important aspect of simulations is the extent to which they correspond to the geometry and properties of the magnetosphere. Disturbances starting near the subsolar point can grow as they propagate back to the flanks of the magnetosphere, where the non-linear stage of evolution is most often compared to experimental measurements. As simulations incorporate more realistic geometries they become more and more applicable to the interaction of the solar wind with Earth's magnetosphere.

Recent simulations have clarified the effect which magnetic shears have on the boundary stability. Miura (1995a) used a two-dimensional code to study northward or southward magnetosheath (IMF) fields outside a northward directed magnetic field in the magnetosphere. This entails a field rotation at the magnetopause for the second case. In this situation, a northward directed IMF B_z is more favourable to the growth of the instability than a southward B_z. When B_z is not directed due north, a slow-mode rarefaction region forms inside the boundary. Similarly, Thomas (1995) used a 3-D hybrid code to demonstrate that even small magnetic field rotations across the boundary layer inhibit the instability and reduce its non-linear growth.

Non-convective KHI has been treated by MHD simulations, imposing periodic boundary conditions including a northward-southward shear of the magnetic field (for a review see, *e.g.*, Miura, 1995b). The convectively growing case has been treated in open boundary systems (Wu, 1986). Most of these simulations are based on solutions of the ideal MHD system of equations in two dimensions.

The 2D-approach seems to be reasonable for application to the magnetopause, but local inhomogeneities and the nonlinear evolution might impose a need for 3D-simulations (Thomas, 1995; Siregar *et al*., 1994; Roberts and Goldstein, 1998). On the other hand, the ideal MHD treatment has a number of deficiencies in so far as it does not contain any transport parameters and thus gives information only on momentum transport. The evolution of steep gradients during the nonlinear stages of such simulations shows their limits, because, strictly speaking, in order for the theory to be valid the allowed gradient lengths must greatly exceed the largest ion gyroradii. But it is not entirely clear whether, for reasonable parameter combinations at the magnetopause, the nonlinear state of the instability can be achieved.

The effect of the magnetic field on the KHI is complex. The ideal linear theory and 2D-simulations suggest that shear flows perpendicular to $\mathbf{B}$ in high-β plasmas are more strongly unstable than are shear flows parallel to $\mathbf{B}$. This is due simply to the fact that bending field lines is much more difficult than compressing them. The parallel fields stabilise the instability by limiting its growth. However, simulations show that the nonlinear evolution differs from the predictions of linear theory. Thomas (1995) cautioned that the results might be affected by the limited mode spectrum used, but 3D-studies by Siregar *et al*., (1994) of the kindred vortex street flow showed that 3D secondary instabilities are strong without the field transverse to the flow and almost nonexistent with it (see Figure 5.15). Secondary instabilities arise in fields already perturbed by the KHI (Metcalf *et al*., 1987). Thus it seems likely that the ordering effect of the magnetic field enforces an approximately two-dimensional state, and the maximum growth rates obtained in this state can adequately represent the situation. Roberts and Goldstein (1998) have tried to produce genuine 3D effects by varying the background density and fields transverse to the flow, using Alfvén waves to excite the instability. Here again, however, the flow has generally been characterised by what look to be ordinary 2D KHI structures of limited transverse extent, with the transverse structure merely representing changes from one region to the next. There may yet be situations in which 3D effects are significant, but they are likely to occur when the geometry is complex and the instability tends to be suppressed due to the necessity to bend the field.

Recent hybrid simulations which use an ion particle code and fluid electrons (Thomas 1995; Fujimoto and Terasawa, 1994) have also treated ion mixing across the boundary due to microscopic effects and the breakdown of the ideal fluid approach. Fujimoto and Terasawa (1994) found that the KHI in an uniform plasma produced enhanced mixing inside the vortices and identified the mixing layer with the LLBL. However, Fujimoto and Terasawa (1995) showed that an inhomogeneous background field reduces the ion mixing, particularly when the magnitudes of the fields differ across the boundary. Thus the influence of the instability on the growth of the LLBL may not be as great as at first thought.

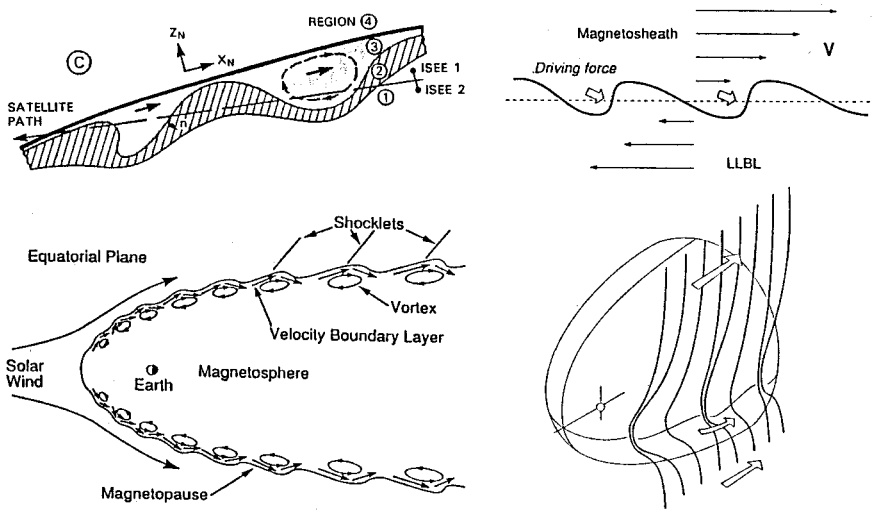

Figure 5.15. Schematic of the wavy magnetopause under conditions when the KHI evolves. *Upper left*: Visualisation of undulatory motion in the LLBL as suggested by ISEE 1 & 2 measurements (Sckopke *et al*., 1981). The magnetopause is assumed to be smooth and undisturbed in this case, and the KHI evolves entirely in the magnetopause low latitude boundary layer. Regions 1 – 4 denote magnetosphere, inner and outer LLBL, and sheath, respectively. *Lower left*: The corresponding equatorial section of the magnetosphere as inferred from MHD simulations (Miura, 1992) with periodic boundaries. The apparently standing vortices exhibiting sunward flow may not be real and should be observed only in a coordinate system which is co-convecting with the KHI wave structure. *Upper right*: Observed driven KH-vortices. These structures seem asymmetric and steepened (this and below from Chen *et al*., 1993b). *Lower right*: A possible magnetic driver model causing an un-symmetrically steepened KHI vortex.

Complex vortex generation and steep gradients as well as turbulent boundary layer flows had already been observed in fluid simulations, in particular those which included viscosities. As Huba (1996a) has shown, two effects change the ideal KHI picture: (1) The inclusion of finite Larmor radius (FLR) effects causes asymmetric evolution in the nonlinear range and the formation of plasma blobs, altering the growth rate; (2) inclusion of the Hall effect leads to similar asymmetries. In addition, coupling of the KHI along the field lines to the ionosphere causes chaotic evolution and turbulence instead of single mode excitation (Keskinen and Huba, 1990; Keskinen *et al.*, 1988).

A 2D-full particle three-velocity simulation has been reported by Wilber and Winglee (1995) which is promising as a first step towards a more precise kinetic picture. The result of this simulation was that the non-thermal differences in the electron and ion motions lead to plasma mixing and transport in the KHI. Discrete intense current layers form at steep gradients; this confirms the fluid simulations of Miura (1982) and Wu (1986) and extends them to narrower scales. The electron contribution is that the plasma generates tongues that penetrate the field region

and may decouple from the plasma source region, in this case the magnetosheath, forming drops. In addition there are asymmetries between dawn and dusk as inferred by Huba (1996a). One may conclude that the microscopic dynamics has a strong effect on plasma mixing driven by the KHI.

5.5.3. PREDICTIONS AND TESTS

A strongly-sheared dense plasma flow transverse to weak magnetic fields favours the development of the Kelvin-Helmholtz instability. These criteria allow us to make definite predictions concerning the locations and conditions under which the instability is expected.

The most straightforward predictions concern the dependence of the KHI on the velocity shear and solar wind conditions. First, the instability should evolve more likely during intervals of enhanced solar wind velocities and densities, where the latter dependence comes in through the Alfvén velocity. The KHI should also be more likely to occur at greater distances downstream from the subsolar magnetopause, because both magnetosheath and LLBL velocities increase in the antisunward direction. There is another reason why it should be easier to observe the instability further down Earth's magnetotail: its amplitude grows convectively with time, equivalent to downstream distance. Sibeck *et al*. (1987d) reported a statistical study of ISEE-3 magnetopause crossings in the distant magnetotail, which showed that the frequency of crossings per day increases with increasing solar wind velocity. Seon *et al*. (1995) obtained similar results indicating that enhanced solar wind velocities favour wavy motion of the near-Earth magnetopause.

Secondly, the instability should be more likely on the equatorial than the polar magnetopause, because equatorial magnetospheric magnetic fields generally are transverse to the magnetosheath flow, whereas polar magnetic fields are parallel or antiparallel to the flow. Furthermore, the equatorial magnetic field strength is generally weaker than that at high latitudes and therefore less able to stabilise the instability. Boller and Stolov (1973) reported early studies which established that the instability criteria could be satisfied on the near-Earth flank magnetopause. Seon *et al*. (1995) looked for, but found no evidence for, this effect.

If the dawn- and dusk-flanks of the magnetopause are taken as the most likely sites for the instability, strongly northward or southward IMF orientations would be expected to favour the development of the instability. Magnetosheath magnetic fields with these orientations would be transverse to the plasma velocity and therefore be unable to stabilise the instability. If the magnetic field rotates from northward to southward orientations across the magnetopause, the intermediate orientation may stabilise the magnetopause (Miura 1995a, b).

Alternatively, conditions for the instability may always be ripe on the inner edge of the LLBL, where the flow shear is always transverse to the magnetospheric magnetic field lines. Ogilvie and Fitzenreiter (1989) have tested the in-

stability criteria at the inner edge of the LLBL and shown that it was satisfied on days when boundary waves were observed. An occurrence of the instability at the inner edge of the LLBL may provide a natural explanation for the plasma blobs frequently seen within the flank LLBL during periods of northward IMF orientation (Sckopke *et al*., 1981; Chen *et al*., 1993b).

A thinner LLBL always favours the occurrence of the instability, since it implies a greater plasma velocity shear across the magnetopause. Some observations indicate that the LLBL is thicker during periods of northward IMF orientation (*cf.* Mitchell *et al*., 1987), although this has yet to be conclusively demonstrated using multiple spacecraft observations.

The instability generates quasi-periodic waves on the magnetopause or on the inner edge of the LLBL which move antisunward with the magnetosheath/LLBL flow. Because wavelengths are on the order of the boundary layer thickness (0.5 R_E) and the waves travel antisunward at magnetosheath velocities (200 km s^{-1}), expected periods are on the order of 5 – 10 min. The waves may be detected as periodic oscillations in the magnetopause normal, calculated by minimum variance analysis. Such waves have been observed on numerous occasions (*cf. e.g.*, Aubry *et al*., 1971; Chen *et al*., 1993b). Wavy magnetopause motion produces characteristic flow patterns in the adjacent magnetosheath which can be observed by plasma instruments located at distances removed from the boundary. It seems likely that the instability could be distinguished from other non-periodic sources of magnetopause motion because it should produce quasi-periodic waves, whereas the other mechanisms (*e.g.*, pressure pulses and FTEs) produce isolated impulsive events (Song *et al*., 1994). But in the absence of additional positive identification we cannot yet rule out the possibility of such periodic patterns being generated by other mechanisms, such as large amplitude waves generated deep in the magnetosheath and convected to the magnetopause. Such waves may pile up there or become resonantly amplified and even become transformed across the magnetopause.

There are a number of other predictions which are more subtle or more difficult to observe: The Kelvin-Helmholtz instability is a macro-instability that, in its nonlinear evolution, locally causes steep plasma and field gradients which may trigger micro-instabilities. In such regions one expects that the diffusivity increases which, in combination with deformation of the magnetic field, may lead to the ignition of reconnection. This should contribute to enhanced local mass transport, ion mixing, plasma acceleration and dissipation of flow and magnetic energy. Furthermore, the effects of the Kelvin-Helmholtz disturbances can be felt at diminishing amplitudes with increasing distance from the magnetopause. The instability may be capable of transporting plasma away from the immediate vicinity of the magnetopause. Correlations between plasma profiles across the flank boundary layer, oscillations of the magnetopause, and ELF magnetic wave spectra are needed to judge the relevance of the KHI plasma transport.

Measurement of the plasma flow fluctuations (after subtracting the average

bulk flow speed) in the flank LLBL can give indication of plasma flow patterns caused by wavy motions. Here the difficulty arises that determination of the flow patterns depends on the reference system. Hence one needs multi-spacecraft measurements to determine the wave k-vector. But not all waves are KH waves. Hence, discrimination requires further arguments. FLR and Hall effects are expected to produce asymmetries in the evolution of the instability on the dawn and dusk flanks (Huba, 1996a,b; 1994), although these predictions have not been tested observationally. Ionospheric coupling causes an evolution of turbulent spectra in the instability. The test of this prediction is to look for power law spectra in the ELF magnetic and velocity fluctuations. It requires precise measurements of the plasma moments.

5.6. Impulsive Penetration

5.6.1. INTRODUCTION

Lemaire and Roth (1978) introduced the concept of magnetosheath plasma elements with excess momentum penetrating impulsively through the magnetopause into Earth's magnetosphere as a consequence of fine structure in the IMF and solar wind plasma, in an effort to explain plasma populating the magnetospheric boundary layer on closed field lines. 'Blobs' of high-density magnetosheath-like plasma frequently appear to be embedded in the less dense background plasma of the LLBL (*e.g.*, Lundin, 1988; Woch and Lundin, 1992b).

At the end of the seventies, laboratory experiments had already proved that (unmagnetised) plasma blobs impulsively injected across homogeneous and inhomogeneous magnetic fields, could freely propagate across magnetic field lines connected to insulating walls (Bostick, 1956; Baker and Hammel, 1965; Demidenko *et al.*, 1969, 1972). An explanation of these laboratory observations was provided by Schmidt (1960). In Schmidt's theory the motion of individual particles in a collisionless plasma blob is considered in the guiding centre approximation and in the low-β limit. Because of the large value of the dielectric constant ($\approx 10^4 - 10^5$ in space plasmas), collective polarisation effects are important. A magnetised plasma element, called 'plasmoid' by Bostick (1956), impulsively injected into a magnetic field can propagate easily across the field lines by electrically polarising in the direction perpendicular to both the magnetic field and the plasma velocity. The electric field thus produced leads to an $\mathbf{E} \times \mathbf{B}$ drift.

5.6.2. PENETRATION THEORY

Assuming that induced electric fields are small, Lemaire (1985b) pointed out that Schmidt's theory can be generalised to a high-β diamagnetic plasmoid if the magnetic field distribution used to derive the particle drifts is the sum of the external

and diamagnetic fields associated with all local and distant currents. That a high-β plasmoid can penetrate across an inhomogeneous magnetic field by means of $\mathbf{E} \times \mathbf{B}$ drift resulting from the self-electric polarisation was illustrated already by Demidenko *et al.* (1969), with parameters in some of their experiments being $\beta \approx 2-3$ ($n \approx 5 \times 10^{14}\,\mathrm{cm}^{-3}$, $v_0 \approx 50\,\mathrm{km\,s}^{-1}$, $B \approx 5 \times 10^{-2}$ T).

Lemaire (1985b) generalised Schmidt's theory to the case of plasma propagation across the sheared magnetic field at the magnetopause. When the direction of the external magnetic field rotates by an arbitrary angle across the magnetopause it was argued that the polarisation electric field inside the plasmoid rotates by the same angle, with the result that $\mathbf{E}$ and $\mathbf{B}$ remain orthogonal to each other.

Adiabatic Braking

Weakly diamagnetic plasmoids are decelerated when they penetrate into the magnetosphere. The reason is that the average magnetic moments of ions and electrons in the plasmoids are adiabatically invariant. The deceleration is proportional to the gradient of the magnetic field intensity and does not depend on the angle of rotation of $\mathbf{B}(x)$ across the magnetopause. Adiabatic deceleration will eventually stop the plasmoid (Demidenko *et al.*, 1969). An estimate of the average penetration distance resulting from adiabatic braking requires knowledge of $\nabla B(x)$ as well as of the statistical distribution of the excess momentum density.

Non-adiabatic Braking

Plasmoids also decelerate non-adiabatically via dissipation of their kinetic energy by Joule heating in the resistive cusp ionosphere (Lemaire, 1977; Lemaire and Roth, 1978). For a large transverse (height-integrated) Pedersen conductivity, Σ_p, the polarisation electric field inside the moving plasma element (which keeps it moving) as well as the dipolar electric field just outside in its surrounding (which deflects the magnetospheric plasma around the intruding plasmoid) are short-circuited. This is not immediate since any potential difference is initially communicated to the ionosphere by hydromagnetic waves that travel along the geomagnetic field lines at the Alfvén velocity.

Using reasonable solar wind parameters ($n = 5\,\mathrm{cm}^{-3}$, $v_{sw} = 400\,\mathrm{km\,s}^{-1}$) the penetration velocity (normal to the magnetopause) of a plasma element with an excess density of 5% is typically $20\,\mathrm{km\,s}^{-1}$ (assuming conservation of the excess momentum density as in Lemaire (1977) and Lemaire and Roth (1978)). This holds under the assumption that the plasma element (crossing the bow shock or internally generated in the magnetosheath) maintains its coherence until it hits the magnetopause. Regarding magnetic field dips observed in the outer magnetosphere as diamagnetic effects associated with the intrusion of magnetosheath plasma blobs, Lemaire (1977) deduced a mean distance of penetration of about 13 000 km. Then, considering that a plasma element with a typical length scale of 10 000 km is at $\sim 10\,\mathrm{R_E}$ when it penetrates through the magnetopause, Lemaire

(1977) was able to give the order of magnitude for a characteristic deceleration time, τ, based on the non-adiabatic braking, as well as an approximate value of Σ_p. He found $\tau \approx 30$ min. The value he obtained for Σ_p (≈ 0.2 Siemens) is close to the usual value given for the high latitude regions of the dayside ionosphere.

Effects of Interplanetary Magnetic Field

The adiabatic braking of weakly diamagnetic plasmoids penetrating into the magnetosphere only depends on the gradient of the magnetic field intensity. However, the orientation of the interplanetary magnetic field (IMF) may also play a role in modifying the penetration velocity of high-β plasmoids because the latter have an intrinsic magnetisation. A diamagnetic plasmoid intruding into the magnetosphere can be accelerated or decelerated depending on the orientation of its magnetic moment $\mathbf{M}$ with respect to the dipole moment of the geomagnetic field. Following Lemaire and Roth (1991), this effect results from the magnetic force $\nabla(\mathbf{M} \cdot \mathbf{B}_{\mathrm{E}})$ exerted by the geomagnetic field $\mathbf{B}_{\mathrm{E}}$ on the magnetic dipole moment $\mathbf{M}$ of a 3-D plasmoid. The strength of this dipole-dipole interaction force is an increasing function of the plasma beta.

The intrinsic magnetic moment of a magnetosheath plasmoid points in the direction opposite to the ambient IMF. Therefore the direction of the magnetic force acting on a high-β plasmoid intruding into the magnetosphere (*i.e.* the direction of its acceleration) depends on the impact location on the magnetopause surface and on the orientation of the IMF in the nearby magnetosheath. For an antiparallel IMF component with respect to the magnetospheric field the magnetic force points towards Earth and acts to increase the velocity of intruding plasmoids. For a parallel IMF component the magnetic force is reversed and acts to decrease the entry velocity.

5.6.3. DISCUSSION

As yet, impulsive plasma penetration theory has not been developed fully. Only qualitative predictions have been made. However, the basic description of the physical mechanism setting up the polarisation electric field within a solar wind plasmoid and permitting it to penetrate and propagate into the geomagnetic field is well established theoretically (Schmidt, 1960; Peter and Rostoker, 1982; Treumann and Häusler, 1985) and is supported by laboratory experiments even in the case of high-β plasmoids (Baker and Hammel, 1965; Demidenko *et al.*, 1969, 1972).

When a high-β plasmoid (charge-neutralised ion beam with $1 < \beta < 400$) is injected into a magnetised plasma the polarisation electric field may be shorted to a degree that increases with increasing background plasma density (Hong *et al.*, 1988). For a background density on the order of the plasmoid density or less – a situation similar to the case of a solar wind plasmoid injected into the

magnetosphere – there is little de-polarisation and the plasmoid is not deflected. The experiments of Hong *et al.* (1988) also show that the magnetic field rapidly diffuses into the ion beam. This process is accompanied by a small diamagnetism. However, large-gyroradius beams ($R < r_{ci}$) limit the diamagnetic effect. In the opposite case $r_{ci} < R$ slower diffusion of the ambient magnetic field is found (Wessel *et al.*, 1988).

The observations of the repulsion or attraction between laboratory plasmoids (Bostick, 1956) support the dipole-dipole interaction between Earth's dipole moment and that of a solar wind diamagnetic plasmoid penetrating impulsively into the magnetosphere (Section 5.6.2).

Schindler (1979) conducted a formal theoretical treatment of the impulsive penetration process for a two-dimensional geometry. On the basis of ideal MHD, Schindler concluded that infinitely long cylindrical filaments, with even a small initial velocity, can enter the magnetosphere provided the magnetic fields in the magnetosheath and in the magnetosphere are either parallel or antiparallel. For oblique angles between the fields he predicted that a filament with excess momentum density is decelerated due to a repelling force arising from the piling up of magnetic flux in front of the filament. He also argued that the requirement of strictly aligned fields is weakened if the effects of non idealised MHD, such as a finite resistivity, are included. A qualitative discussion of these non-ideal MHD effects suggested that penetration may be possible for oblique angles between the magnetic fields, provided the filament has sufficient excess momentum to trigger spontaneous merging of magnetospheric field lines behind the partly penetrated filament.

Alternatively, even a plasma blob with a weak excess momentum is allowed to penetrate because the coupling with the background plasma may be achieved by weak electrostatic double layers created along the magnetic field lines crossing the plasma blob (Roth, 1995).

Numerical Simulations

Schindler's results were confirmed by a two-dimensional resistive MHD simulation (Ma *et al.*, 1991): a field-aligned magnetosheath filament oriented at an oblique angle with respect to the magnetospheric field can penetrate only when its initial kinetic energy density exceeds by a factor of 50 the magnetic energy density in the transverse component of the magnetospheric magnetic field. This result means that, for typical magnetopause parameters, the filament penetration is possible only if the angle between the fields is less than $\approx 5^\circ$. However, as the authors noted, in the 3-D case, the condition might be considerably less restrictive. They also recognised that non-MHD effects are likely to play an important part in the process of impulsive penetration.

Two-dimensional hybrid simulations with particle ions and fluid electrons were used to simulate impulsive plasma penetration through a tangential dis-

continuity magnetopause of finite thickness (Savoini *et al.*, 1994). Simulations were performed with strictly parallel or antiparallel magnetic fields in the magnetosheath and in the magnetosphere. Compared to the resistive MHD calculations of Ma *et al.* (1991) these hybrid simulations revealed important differences: the development of twin vortices in the magnetosphere due to the filament motion, in the antiparallel case a strong distortion of the filament shape by these vortices and a transverse deflection of the filament (instead of the straight displacement obtained in Ma *et al.*, 1991), and the breakup of the filament into smaller parts leading to isolated islands of magnetosheath-like plasma and field in the magnetosphere on the order of the ion gyroradius.

It is important to note that the hybrid and MHD simulations (including ideal MHD calculations of Dai and Woodward (1994, 1995) and Hall MHD calculations reported by Huba (1996b), are two-dimensional and have mainly been performed for the highly unrealistic case of strictly parallel (or antiparallel) fields. The results of these numerical simulations are therefore not fully representative of the solar wind-magnetosphere interaction, since plasma density irregularities are three-dimensional entities. For example, within a 2-D infinitely long filament there is no magnetic coupling between the inside and the outside, in contrast with a real 3-D plasmoid. Furthermore, numerical simulations do not consider any microscale thermoelectric effects (Lemaire and Gringauz, 1998).

Solar Wind and Magnetosheath Plasmoids

It is known from radio scintillation measurements (*e.g.*, Woo and Armstrong, 1979) that plasma density fluctuations spanning an extensive range of spatial and temporal scales are always present in the solar wind. Near the heliospheric current sheet these density fluctuations are high and highly variable (Woo *et al.*, 1994). Enhanced density fluctuations can be either of solar wind origin (Watanabe and Schwenn, 1989) or internally generated in the interplanetary medium (Ananthakrishnan *et al.*, 1980).

Figure 5.16 shows a direct measure of the density fluctuation as a function of the mean electron density for a three hour period in 1978 ($\langle n \rangle$ less than $10\,\mathrm{cm}^{-3}$), and nearly a whole day in 1981 ($\langle n \rangle$ larger than $10\,\mathrm{cm}^{-3}$). The figure shows that the relative density fluctuation $\Delta n/\langle n \rangle$ is high and independent of the mean density. During the intervals studied it varies over the range $0.04 < \Delta n/\langle n \rangle < 0.09$, with a most probable value of ~ 0.05. It may be related to the proton temperature. Celnikier *et al.* (1987) also noticed that the most important contribution to the overall fluctuation level comes from the high frequencies (smaller spatial scales).

Celnikier *et al.* (1987) found no evidence of substantial elongation of the density irregularities along the field direction. The authors also quoted that, in at least part of their data, fluctuations in density and fluctuations in magnetic field strength were anti-correlated over a very large range of spatial scales. This would be an indication that solar wind irregularities are diamagnetic entities which are not

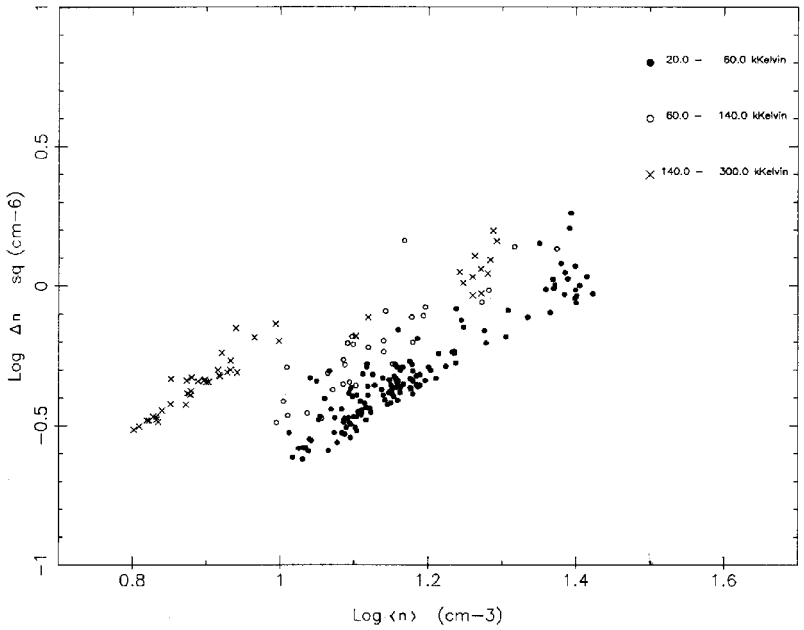

Figure 5.16. Log (fluctuation in electron density) as a function of log (mean density) obtained from the ISEE 1–2 wave propagation experiment. The fluctuation in electron density was estimated by integrating the smoothed four minute averaged power density spectra from 0.019 Hz up to 16 Hz. With an average solar wind speed of $\approx 450\,\mathrm{km\,s^{-1}}$ the spatial scales of the density fluctuations are in the range of 30 – 25 000 km. The filled circles pertain to a proton temperature range of 20 to 60 K, the open circles to a range 60 to 140 K and the crosses to temperatures exceeding 140 K (from Celnikier *et al.* (1987)).

necessarily strongly elongated along the IMF and may resemble the 3-D plasma-magnetic entities called 'plasmoids' in laboratory experiments (Bostick, 1956). There are, however, recent observations suggesting that small-scale ($3-4R_E$) solar wind plasma features are relatively well correlated over distances comparable to magnetospheric dimensions, particularly during periods of enhanced solar wind variability (Paularena *et al.*, 1998). To be fully relevant in the context of impulsive penetration, these results should, however, be complemented by studies of plasma correlations at even smaller spatial scales.

In situ measurements in the solar wind at 1 AU have also shown that the relative density fluctuations are more intense downstream of interplanetary shocks (Huddleston *et al.*, 1995). Such a relative increase in the density fluctuations also occurs in Earth's magnetosheath, downstream of quasi-perpendicular shocks (Lacombe *et al.*, 1997). Furthermore, small-scale irregularities (on the order of 1000 km) attributed to drift mirror waves are observed in the magnetosheath (Hubert *et al.*, 1989).

Theoretical Verification

For impulsive penetration to occur, plasma elements with an excess momentum must survive in the magnetosheath until convected toward the magnetopause, avoid draping around the magnetopause by convective dilution, and keep enough excess momentum to hit the magnetopause.

Some additional points will help clarify the above requirements. Bow shock perturbations by interplanetary disturbances have been studied by Völk and Auer (1974) for the special case of the 1-D interaction of a planar tangential discontinuity with a perpendicular shock. Extensions to the case of a finite 3-D plasma blob and arbitrary IMF orientation remain to be done before one can evaluate the possible significance of such studies on the motion of a blob through the magnetosheath. In a gas dynamic model (Spreiter *et al.*, 1966), a plasma element crossing the bow shock with an excess density would follow the same streamline trajectory as if it were embedded in a density-enhanced but uniform solar wind flow, pushing the magnetopause towards Earth. The plasma blob hits the magnetopause only if its streamline cuts across the boundary. Whether or not this will happen depends on the excess momentum and distance from the bow shock traversal. It is expected that solar wind blobs hitting the magnetopause on the average have the largest normal impact velocity near the subsolar point. They can hit the flanks of the magnetopause only if they have sufficient excess density.

Plasma elements with $\Delta n < 0$ are not able to reach the magnetopause position. Indeed, in a gas dynamic approach they would follow the same streamline trajectories as if they were embedded in a density-reduced but uniform magnetosheath plasma deflected along the magnetopause, which is necessarily displaced outwards. Therefore, the magnetopause acts like a rectifier allowing only plasma density enhancements to penetrate into the magnetosphere.

For non-sheared magnetic fields, theory and laboratory experiments as well as numerical simulations have demonstrated that impulsive penetration necessarily takes place. For sheared fields, impulsive penetration has been treated theoretically only in very basic approximations. More realistic approaches are difficult to study and require non-MHD three-dimensional numerical simulations for configurations that include sheared fields. It would also be interesting to modify the magnetic field distribution in laboratory experiments to simulate situations where the magnetic field is sheared.

Experimental Verification

There are no direct observations of impulsive injection near the magnetopause. Lühr and Klöcker (1987) and Treumann *et al*. (1990) found a 'magnetic hole' containing dense plasma just inside the magnetopause, but they interpret it in a different way. Observations of magnetospheric and ionospheric signatures of impulsive penetration have been reported, however, as reviewed by Lundin (1988) and Lemaire and Roth(1991)). Since some of these observations can also be ex-

plained in the framework of transient reconnection (FTE), Kelvin-Helmholtz instabilities, or solar wind pressure pulses, they do not provide indisputable evidence for the mechanism. Note, however, that a careful analysis of transient penetration signatures of plasma with magnetosheath origin observed by Viking in the dayside magnetosphere at auroral latitudes has led Woch and Lundin (1992b) to conclude that impulsive penetration was the most reasonable interpretation of their observations (excluding any role for reconnection in the entry process).

Future experimental verification should concentrate on the detection of plasma blobs with excess density and small size and the study of their evolution from the solar wind to the magnetopause, including their possible dilution in the magnetosheath. The WHISPER experiment on the Cluster spacecraft (Decreau *et al.*, 1997), with its capability to measure the absolute value of the total density at four points, will provide information about the structure, the scale size and velocity of plasmoids in the solar wind, magnetosheath and flanks of the low-latitude boundary layer.

5.7. The Special Role of the Cusp

5.7.1. INTRODUCTION

Evidence for magnetosheath plasma entry at high latitudes on the dayside was provided by low-altitude polar orbiting satellites (*e.g.*, Burch, 1968; Heikkila and Winningham, 1971; Frank, 1971). Statistical studies suggested a narrow region near local noon with the magnetic field topology forming a cusp (or 'throat') - called the 'polar cusp'. This polar cusp produces persistent features in low-altitude data, having a somewhat larger extent than would be implied from magnetic topology considerations. For a while, it was debated whether it had the shape of a *cusp* or a *cleft*.

High-altitude satellite observations (HEOS–2, Prognoz–7, Hawkeye) led to the identification of the high-altitude counterpart of the low-altitude cusp/cleft regions. Three magnetopause boundary layer regions have been identified in the HEOS-2 data: The entry layer (Paschmann *et al.*, 1976), which is a region of diffusive, turbulent entry of magnetosheath plasma onto field lines that map to the low-altitude cusp; the plasma mantle (Rosenbauer *et al.*, 1975), which is located on field lines where the injected magnetosheath plasma continues tailward; and the exterior cusp (Sckopke, 1979), which constitutes a pocket of hot 'stagnant' and possibly turbulent plasma outside the magnetopause. Frequently no well defined current sheet could be identified in the distant cusp data (*e.g.*, Haerendel *et al.*, 1978; Lundin, 1988). This may suggest that it is a flow boundary rather than a magnetopause current sheet that separates the magnetosheath from the magnetosphere in the cusp.

A distinguishing difference between the reconnection process and other processes governing magnetosheath plasma access to the magnetosphere (via direct entry in the cusp or by diffusion and impulsive penetration) is that the latter produce local effects in the magnetospheric boundary layer and its coupling to the ionosphere. In the reconnection model, magnetic field lines merge on the dayside magnetopause and convect across the cusp into the mantle (*e.g.*, Dungey, 1961; Lockwood and Smith, 1992; Onsager *et al.*, 1993). In such a model, the cusp position and extent depend strongly on the IMF. In non-reconnection models the cusp position and extent are less sensitive to the IMF, but depend more strongly on the solar wind ram pressure. The reconnection model has already been discussed in Section 5.2. In this section we describe an alternative model that is based on gas dynamics.

5.7.2. GAS DYNAMIC MODEL OF THE CUSP

Yamauchi and Lundin (1994) proposed an analogy between the cusp and a de Laval nozzle with solar wind plasma entering the entry layer/exterior cusp and exiting to the plasma mantle. The motivation for proposing the dynamic cusp model is based on three main observational characteristics obtained from low-, and mid-altitude satellites:

- The cusp is a persistent feature, frequently transient in nature and changing in latitude and longitude with respect to *e.g.*, the IMF - but also stably positioned for hours.
- The cusp is influenced strongly by the solar wind dynamic pressure - in width, latitude as well as longitude.
- The cusp is not a ‘singularity’, but rather a locus of solar wind plasma that expands/diffuses deeply into neighbouring regions of the dayside magnetosphere on closed field lines. The injected plasma may stagnate (in the subsolar region) but appears predominantly to preserve a flow in the tailward direction (flow channel).

Fig. 5.17 illustrates qualitatively the topology of the plasma access region (left) with the de Laval velocity and pressure relations (right). In gas dynamics, the de Laval nozzle is a special case based on a constricted flow channel. For the cusp the constriction is thought to be due to a combination of the magnetic field (cusp) geometry and local mass-loading that may inhibit plasma from expanding freely into the nozzle. The de Laval nozzle is generally used to convert high pressure to supersonic outflow speed. In the cusp, the high plasma pressure built up in the dayside magnetosheath is eventually converted into supersonic flow in Earth’s plasma tail.

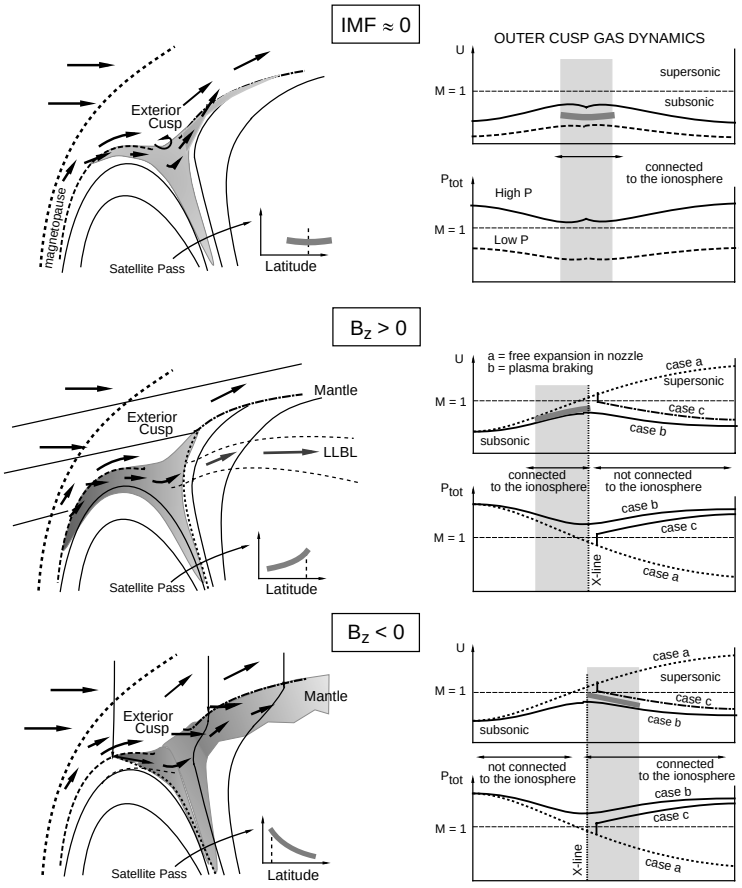

Figure 5.17. Gas dynamic/flow model for steady-state magnetosheath plasma injection into the plasma mantle for various IMF conditions. In the left part of the figure, arrows indicate the local flow direction. Shaded areas are regions where the solar wind plasma has direct access to the cusp. In the right-hand diagrams, the abscissa for the speed u and total pressure p_{tot} marks the access route from the dayside magnetosheath, through the cusp, into the nightside boundary layer/magnetosheath. For northward (southward) IMF the X-line is on the polar (equatorward) edge of the cusp. Symbols *a, b, c* correspond to three different cases: velocity increasing up to supersonic speed, increasing and subsequently decreasing velocity, and the case where a shock is formed ahead of the cusp. Thin arrows indicate the regions that are magnetically connected to the ionosphere. The small inserts show the ion dispersion as a function of latitude at low altitudes (after Yamauchi and Lundin, 1994).

In the gas dynamic model considered, the flow velocity branches off into two regimes, (a) increasing velocity up to supersonic speeds, (b) increasing and subsequently decreasing velocity (Venturi pipe). Eventually, case (a) will apply because plasma escaping from the cusp eventually reaches supersonic speed in the deep tail. The physical reason for the mechanism is that solar wind plasma has access to the cusp nozzle over a wide area, building up plasma pressure in the access

region. The nozzle poses an obstacle that limits plasma expansion until it reaches the deep tail mantle (for $B_z < 0$) where it may flow freely along the magnetic field lines in an expansion fan. The nozzle obstacle has two main causes: the magnetic field geometry (in and out of a converging/diverging cusp), and the momentum transfer between downgoing and mirroring plus upwelling ions.

A third regime (c) exists, provided a new shock is formed ahead of the cusp. The cusp presents an obstacle to the magnetosheath flow, which already at cusp latitudes can have attained supersonic speed again. As noted by Walters (1966), the obstacle need not be solid. A pressure increase due to magnetospheric plasma escaping into the plasma mantle might have a similar effect, by narrowing a local flow passage (or 'stream tube' in fluid dynamics terminology).

The gas dynamic model predicts a spatial ion dispersion signature that resembles the observed ion dispersion that is usually explained in terms of plasma convection. Figure 5.17 illustrates the morphology of steady state plasma access to the cusp for various IMF conditions.

In discussing the gas dynamic model of the cusp it is appropriate to start with what can be termed the 'ground state' of plasma access into the cusp, *i.e.* when the IMF is weak (IMF ≈ 0, top). The electromagnetic influence on the cusp is then negligible and the cusp is controlled by solar wind plasma dynamics. In fact, the existence of a cusp for weak IMF can be considered evidence for steady-state plasma entry into the cusp. A characteristic feature of the cusp for IMF ≈ 0 is the lack of latitudinal dispersion features (*e.g.*, Woch and Lundin, 1992a) and a lack of plasma convection signatures.

The 'ground state' cusp may be considered a diffusive access of solar wind plasma into an open throat to the magnetosheath, with plasma pressure building up in the centre of the cusp and plasma subsequently 'diffusing' into nearby magnetic field lines of the cusp. Depending on the solar wind dynamic pressure, the cusp will move equatorward (high pressure) or poleward (low pressure) as well as increase in width (for increasing pressure). This is in good agreement with the pressure dependence found from low-altitude satellites (Newell and Meng, 1994a).

The 'ground state' cusp may seem unimportant from the solar wind plasma access point of view. Yet, low-altitude satellite observations show that solar wind plasma also has access to the dayside magnetosphere for weak IMF, in particular for increased solar wind dynamic pressure. Observations also show that solar wind plasma diffuses into nearby closed magnetic field lines, setting up a boundary layer. The exact process responsible for such a 'diffusion' is yet to be determined, but the weak magnetic field in the outer cusp may be one important reason for the entry. What is of prime interest for the gas dynamic model of the cusp is rather the plasma transport and the related flow channels.

A characteristic feature of the gas dynamic model is that the plasma always flows tailward in the cusp and the related boundary layers. Only reconnection

can reverse the plasma flow such that it moves sunward. Once entering the outer cusp, plasma will move in various directions (IMF dependent) into the plasma mantle or the LLBL. Observations show that the plasma mantle exists mainly for IMF $B_z < 0$, while it essentially vanishes for IMF $B_z > 0$. Moreover, there are indications that the LLBL near the subsolar region becomes thicker for IMF $B_z > 0$ (Yamauchi et al., 1993b). Thus one would conclude that solar wind plasma entering into the cusp flows into the plasma mantle for IMF $B_z < 0$, but into the LLBL for IMF $B_z > 0$.

For IMF $B_z > 0$ (Figure 5.17, central panel) solar wind plasma enters over a relatively large area of the dayside magnetopause, from the LLBL to the entry region in the vicinity of the cusp. After penetrating/diffusing through the magnetopause on the dayside, the injected plasma first stagnates but subsequently expands towards higher latitudes into the outer cusp. The lowest flow velocities are then in the stagnation point and the highest in the poleward region of the cusp. Notice that the injected plasma is not expected to traverse the poleward boundary of the cusp (X-line) into the lobe/mantle. The tailward flowing plasma may instead expand towards the flanks into the high-latitude portion of the LLBL. Current sheet/reconnection acceleration of plasma may be observed at the poleward X-line (*e.g.*, Woch and Lundin, 1992a).

For IMF $B_z < 0$ (Figure 5.17 bottom) direct access of solar wind plasma into the (northern) cusp, indicated by the shaded area in the U, P diagram, is expected to occur poleward of the X-line, assumed here to be located just equatorward of the cusp. Once ions have entered the cusp, pressure balance conditions imply that an increased total pressure in the poleward section of the cusp proper, partly due to an increased magnetic pressure, corresponds to a decreasing parallel velocity (subsonic case b). A consequence of the magnetic obstacle ('bending the magnetic field lines'), the return flow of sheath ions, and the upflowing ionospheric ions in the cusp, is to prevent solar wind plasma from freely expanding in the near Earth plasma mantle region, thus prohibiting the plasma from reaching supersonic velocities (as in case a). Plasma in the low-altitude cusp must bear the same signature as the high-altitude plasma, *i.e*. a decrease of velocity poleward. Since the effect of the 'magnetic obstacle' will become less further tailward, the mantle plasma should eventually reach supersonic speeds.

The substantial ionospheric ion fluxes found in the plasma mantle (Lundin *et al*., 1982) as well as in the sheath region outside the cusp (Eklund *et al*., 1997) are a crucial element of the Laval nozzle model. Mass-loading due to outflowing ionospheric ions is important in the flow topology of the cusp.

5.7.3. OBSERVATIONS RELATED TO THE GAS DYNAMIC MODEL

Studies by Aparicio *et al*. (1991) and Newell and Meng (1994a) as well as analysis of Viking cusp data show a good correlation between cusp densities and

temperatures and the solar wind Mach number (*e.g.*, Lundin, 1997). Moreover, the dawn-dusk shift of the cusp position is affected by the IMF B_y, and by the east-west flow of the solar wind (Lundin, 1997; Newell *et al*., 1989; Aparicio *et al*., 1991). It is also found that the cusp is continuously open to the solar wind/magnetosheath, independent of the IMF direction.

From an observational point of view the cusp is a persistent feature. In the framework of dayside reconnection this would require the process to operate in a time-stationary fashion. If, however, reconnection becomes bursty (*e.g.*, Smith and Lockwood, 1990; Lockwood, 1995), cusp field lines would be open only for short intervals of a few minutes each. Observations (Sandahl *et al*., 1997) of cusp encounters with durations of longer than one hour seem inconsistent with this view. Thus, whatever the access process is (steady state merging or steady state inflow in the exterior cusp), at times the cusp provides quasi-steady access for the solar wind, which remains for hours.

Mid-altitude observations also suggest time-dependent plasma injection (*cf.* Yamauchi and Lundin, 1994; Norberg *et al*., 1994). In this case the injection features are referred to as the boundary cusp, *i.e.* the observations taking place in a transition region (Kremser and Lundin, 1990) related to a more pronounced energy transfer (*e.g.*, local plasma heating/acceleration) than in the cusp proper. Transient plasma injection, characterised by time dependent features of the ion energy-time spectrograms (Yamauchi and Lundin, 1994), are more easily observed generally at mid and high altitudes (*e.g.*, Viking, DE-1, and Akebono), but have also been observed at low altitudes (Norberg *et al*., 1994). Time-dependent plasma injections have also been observed outside the cusp in the cleft/LLBL (Carlson and Torbert, 1980; Kremser and Lundin, 1990). This kind of plasma injection requires the temporal 'openness' of the magnetopause (Woch and Lundin, 1992b). It also leads to plasma access onto closed field lines where it may serve as a signature (Pottelette and Treumann, 1998) of the injection process during reconnection.

The enhanced access of solar wind plasma into the dayside magnetosphere caused by high solar wind dynamic pressure is most obvious for northward B_z. Reversed convection signatures with equatorward convecting ions are found in the cusp during such periods. Yamauchi *et al*. (1993) reported observations near local noon for $B_z > 0$, which imply stagnant solar wind plasma injection structures. They are characterised by multiple injection structures that may extend up to ten degrees in invariant latitude equatorward of the poleward cusp boundary. They are 'stagnant', because the mean ion energy decreases steadily equatorward, apparently due to cooling of the injected plasma. The overall ion signature resembles that of the ion expansion into the polar cap/mantle. In this process, the dayside LLBL widens substantially for northward IMF (see Figure 5.17, top).

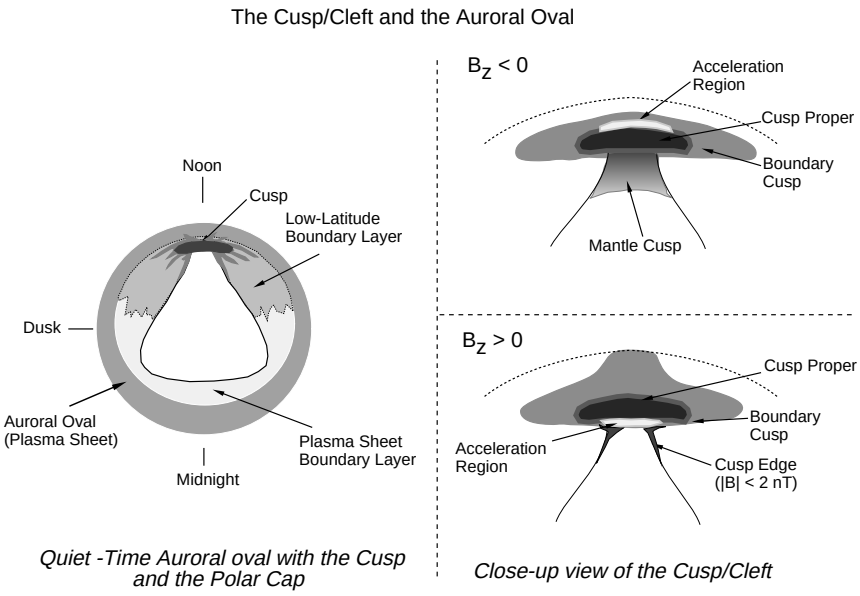

Figure 5.18. *Left*: Summary cartoon of cusp position with respect to the auroral oval and polar cap. *Right*: Close-up look of the characteristic regions inferred from measurements of hot plasma by low- and mid-altitude satellites for negative and positive B_z, respectively (from Lundin, 1997).

5.7.4. CUSP SUMMARY

Figure 5.18 provides a summary of the cusp and cleft morphology based on Viking observations. This figure illustrates the phenomenological features of the cusp and their location with respect to the auroral oval, rather than giving a model of the cusp response to interplanetary disturbances. The left-hand side shows the position of the cusp with respect to the auroral oval, largely inspired by the Tsyganenko model (Tsyganenko, 1987). It is assumed that the polar cap is located well poleward of the continuous oval, as is generally the case for a northward IMF with $B_y \approx 0$ (Jankowska *et al.*, 1990). The cusp is located poleward of the oval. The cleft is the region bounding the cusp equatorward of the polar cap and poleward of the dayside auroral oval in the morning and afternoon sectors. The cleft width and local time distributions depend on B_z (Mitchell *et al.*, 1987). The right-hand side shows a blow-up of the cusp with the various regions identified for northward and southward IMF, *e.g.*, the acceleration region (Woch and Lundin, 1992a) and cusp edge (Yamauchi and Lundin, 1993). The cusp is statistically rather narrow in latitude but elongated in longitude. This elongation grows with increasing solar wind dynamic pressure (*e.g.*, Newell and Meng, 1992). Recent Freja results indicate that the elongation is also present for the instantaneous cusp.

A prominent feature of the cusp region is that the poleward extension, the

plasma mantle, widens for southward IMF and shrinks or disappears for northward IMF. Conversely, the equatorward extension of the cusp shrinks for southward IMF and for northward IMF conditions it expands, covering more than five degrees in invariant latitude. Such a deep protrusion of solar wind plasma into the dayside magnetosphere near local noon (Yamauchi *et al.*, 1993) is difficult to conceive as transport of plasma from the poleward part of the cusp. The alternative is direct access of solar wind plasma through the dayside magnetopause near local noon, or appending solar wind flux tubes to the dayside magnetosphere through reconnection tailward of both cusps, as discussed in Section 5.2.5.

5.8. Summary and Conclusions

In this chapter we have reviewed the processes that are commonly considered to be important for the transfer of plasma across the magnetopause, the predictions from those processes and, where possible, their observational tests.

Magnetic reconnection makes a wide range of predictions for plasma, magnetic field, and energetic particle signatures in the immediate vicinity of the magnetopause and at remote locations in the ionosphere and magnetosphere. Many of those processes have been confirmed experimentally, some even quantitatively. Consequently, there cannot be any doubt that reconnection actually occurs. Since it is the mechanism that naturally predicts the observed dependence of geomagnetic activity on changes of the IMF orientation, a good case can be made that reconnection is the dominant mode for the dynamic solar wind-magnetosphere interaction. But it should be noted that other entry mechanisms, notably impulsive penetration, cusp interaction, and perhaps also diffusion, might show some IMF-dependence as well.

A unique feature of reconnection that sets it apart from all other competing processes (although certainly not proving its dominance) is that it requires the relevant physical processes to take place only in the narrow diffusion region, while its consequences are global: Once the interplanetary and terrestrial magnetic fields become connected, they remain interconnected while being convected with the solar wind along the magnetopause, and plasma continues to enter the magnetosphere by fluid flow. This is in contrast to all other mechanisms: they operate only locally, *i.e.* their occurrence at different locations is essentially uncorrelated.

While it is clear that reconnection does occur at the magnetopause, it is less clear why this is so. There are distinct differences of opinion as to what mechanism ‘thaws’ magnetic flux from the plasma. Prospective agents are anomalous resistivity, electron inertia, non-gyrotropic electron distributions, and the effect of a ‘complex’ equation of state and/or closure for the electrons. From the viewpoint of this book, however, the most significant remaining open question is to quantify the total amount of plasma that is transferred across the magnetopause as a function of solar wind conditions.

Finite Larmor radius effects have been considered, but there is a lack of clear predictions. For example, it remains unclear whether this process predicts greater or lesser plasma entry into the magnetosphere during periods of northward or southward IMF orientation, or how plasma entry depends on position on the magnetopause and solar wind parameters. While it seems certain that particles with high energies successfully gradient-drift into and out of the magnetosphere, the efficiency of this process for particles with thermal energies remains unclear. Drift-entry via polarisation electric fields has been mentioned as a potential entry mechanism, but lacks corroboration from observations.

The theory of diffusive processes is well developed. Since the rate of diffusion is not predicted to depend strongly upon the interplanetary and magnetosheath magnetic field orientation, diffusion is probably not a primary candidate for the dominant solar wind-magnetosphere interaction, but it may be significant for plasma entry during times of northward IMF. Observations during individual magnetopause crossings have been interpreted in terms of local diffusive processes, but further statistical studies are required. Wave amplitudes are usually found to be inadequate to populate the boundary layers, but they seem quite adequate to cause the anomalous resistivity that is needed to ignite reconnection.

Theoretical and numerical simulations of the Kelvin-Helmholtz instability are in a mature state. However, this instability does not directly transfer plasma across the magnetopause unless it reaches a nonlinear stage (which is not likely on the dayside magnetopause). As a result, the Kelvin-Helmholtz instability is certainly not a primary candidate for the dominant mode of solar wind-magnetosphere interaction. When, however, the Kelvin-Helmholtz instability reaches the nonlinear stage, which could occur along the tail-magnetopause, it may cause large-scale eddies to develop. Such eddies may have sharp gradients and couple to microscale effects such as diffusion. In such cases the Kelvin-Helmholtz instability will contribute to local diffusion, but may trigger also local reconnection.

More work remains to be done before impulsive penetration can be established as a significant mode of solar wind-magnetosphere interaction. The model is based on the presumed existence of filaments or bubbles in the solar wind with an excess momentum density. While the solar wind parameters are highly variable, multi-spacecraft observations generally indicate that these variations are planar and extend over great distances. On the other hand, processes that occur at the bow shock may introduce considerable short-scale length variability into the density just before the plasma interacts with the magnetosphere. Whether blob-like structures succeed in crossing the magnetosheath while maintaining their coherence remains to be determined.

The unique conditions governing the polar cusps – weak magnetic field, strongly diverging magnetic field directions, turbulent plasma flows – make the cusp an ideal candidate for direct plasma entry. The complicated nature of the observed cusp signatures and the scarcity of *in situ* observations, however, make

it difficult to decide on the dominating process(es). The cusp plasma certainly populates the open field lines of the plasma mantle, at least for southward IMF, but it is not certain whether it will access the LLBL particularly its closed field line portion. For northward IMF, the situation is more complicated. Low-altitude measurements suggest that, with increasingly northward IMF, access to the LLBL increases while access to the plasma mantle decreases.

From boundary layer observations one obtains a crude empirical estimate of the rate at which solar wind plasma enters the dayside magnetosphere, on the order of $10^{26}\,s^{-1}$. Fluxes observed to escape downstream in the deep magnetotail are as high as $10^{28}\,s^{-1}$ or more (*cf.* Chapters 6 and 7). Reconnection can account for these fluxes, at least for southerly directed IMF. On the other hand, diffusion cannot account for these fluxes unless one assumes the maximum conceivable diffusion coefficient, $10^{9}\,m^{2}\,s^{-1}$, everywhere along the magnetopause. For an average diffusion coefficient more in line with wave observations, the flux would be two orders of magnitude smaller, and thus quite inadequate.

While much of the discussion has focused on the role of the magnetopause as a source region for magnetospheric plasma, observations show that it is also a loss region. As to the loss processes, essentially all source mechanisms discussed in this chapter also can serve as loss mechanisms. Not many quantitative measures of the loss rates are available, however. For reconnection, a crude estimate would indicate that the loss rate of magnetospheric plasma on the dayside is $\approx 10\%$ of the solar wind input rate.

5.9. Future Directions

In this section we discuss future experimental and theoretical work that is needed to improve our understanding of the basis transfer processes and to quantify their contribution to the overall plasma transfer across the magnetopause.

Reconnection. More theoretical work is needed to clarify the relative importance of the different terms in the electron momentum equation (Ohm's law) in the 'thawing' of magnetic flux in the diffusion region. Three-dimensional time-dependent reconnection studies are needed to investigate the role of patchy and transient reconnection. These questions will be answered only by numerical simulations (hybrid or full-particle codes).

A question posed by the *in situ* observations concerns the frequent inconsistency between fluid and kinetic signatures. Furthermore, the *in situ* observations have all been taken *outside* the diffusion region. Measurements *inside* the diffusion region would help to distinguish among the different models of reconnection. The difficulties are threefold. First, the region is predicted to be small in extent along the magnetopause and thus will be missed by most magnetopause traversals. Second, it could be very thin, thus not be resolved in the measurements.

Third, theory has not been developed to a state where quantitative predictions of observable signatures are being made.

An interesting alternative to measurements within the diffusion region could be remote sensing, using ion measurements. In the diffusion region ions will essentially be unmagnetised. As a consequence, their motion will be affected by the electric fields in that region and those effects will remain encoded in the distribution functions once the ions have left the diffusion region.

Once micro-processes in the diffusion region have been identified, one might hope to answer the important question whether there is a relation between the micro-processes and their global consequences, such as the overall mass transfer rate. The quantification of the plasma transfer rate requires direct *in situ* measurements of the local reconnection rate and on the instantaneous extent and location of the X-line(s). Multi-point *in situ* measurements and imaging techniques are needed to settle these questions. But low-altitude measurements will remain an important means to monitor transients in reconnection rates. A goal would be to test whether or not there is a one-to-one relationship between the cross-tail electric potential and the global mass transfer rate across the magnetopause.

Finite-Larmor-Radius Effects. In order to investigate the importance of these effects, a separation of the contributions to the stress tensor of the FLR- and non-FLR effects is required. This requires analysis of high-resolution measurements of the three-dimensional particle distribution function. Single-particle theory can give only a hint concerning the importance of FLR effects. A kinetic theory of the inhomogeneous problem is needed. If FLR effects are important, one expects the transfer process to be dependent on particle energy and mass. As yet neither effect has been studied systematically. To support the measurements, it would be important to include the heavier particles in plasma kinetic simulations

The role of electric polarisation drift effects have received little attention but deserve further investigation, in particular when observations indicate that temporal variations in the electric convection field indeed occur.

Diffusion. The theory of the diffusion process is still open to many improvements. Such improvements should concentrate on the importance for diffusion of the different terms in Ohm's law. It is clear that for the conditions at the magnetopause and in the LLBL, inhomogeneity on the scales of the ion gyroradius and ion inertial length, respectively, must be taken into account. The main activity should concentrate on numerical simulations. They must account for the proper boundary conditions (shear in the magnetic field and flow, density and temperature gradients, composition gradients, heat fluxes and heat flux gradients, turbulent sheath plasma) and should not be restricted to 2-D. Only 3-D simulations can identify the interacting wave modes. Finally, modern developments in statistical mechanics

including Lévy flight dynamics of particles in the presence of turbulence seem to be promising.

Another important theoretical prediction is that macro-instabilities like the Kelvin-Helmholtz instability or eddy turbulence may couple to micro-instabilities, *i.e.* generate conditions under which micro-instabilities may evolve locally. If this occurs, diffusion may concentrate in spatially localised regions, which serve as small-scale sources for the LLBL plasma component. Steep gradients generated by the KHI are good candidates.

Much of the controversy regarding the importance of diffusion may be due to the limitations in present measurements and analysis. There is a need for measurements of spatial density profiles across the magnetopause and boundary layer. For reasonably time-stationary conditions, those profiles could be used to determine diffusion coefficients. When it is possible to construct diffusion coefficients, it is important to identify the energy range and species to which they refer, because diffusion can be species- and energy-selective. Multi-spacecraft missions, or entirely new methods based on techniques such as imaging, tomography, or radio sounding, will definitely improve the situation.

Three-dimensional wave forms measured in high space-time resolution are essential for assessing the importance of diffusion. They should provide not only information about the relevant wave modes but also about their non-linear evolution, saturation intensities, spatial distribution and coupling to the particle component as well as to other modes.

Role of the Kelvin-Helmholtz Instability. The KHI may be one of the macroscopic triggers of diffusion or reconnection. It is not believed that it will lead to transport by itself. Theory and 3D numerical simulations should ultimately clarify whether KHI can evolve on the dayside or flank magnetopause under various boundary conditions (*e.g.*, velocity shear, magnetic shear). Also, it is important to settle the question whether KHI occurs at the magnetopause or at the inner edge of the LLBL. Hybrid simulations with particle ions and fluid electrons can give information about the kind of phase space distributions needed to distinguish KHI from FTEs. Full particle codes should be used in simulations in order to assess the importance of microscopic effects on the KHI.

Another question is whether and how KHI develops into turbulence. If KHI occurs, transport of plasma over the large diameters of the KHI vortices is possible even without diffusive effects. This would then lead to eddy diffusion in the coupling between KHI vortex motion and diffusive effects or even to reconnection on the small scales of the KHI vortices. It is also important to investigate what the effects of plasma composition would be on KHI, its coupling to the ionosphere along the field lines in different places, generation of kinetic Alfvén waves in the KHI vortices, and the resulting parallel electric fields.

Impulsive Penetration. Since this transfer mechanism requires the existence of plasma elements with excess momentum, measurements should try to identify the occurrence of such blobs in the magnetosheath and just outside the magnetopause as well as their appearance inside. Theory should clarify under which conditions plasma blobs can survive over large distances until they reach the magnetopause or if they can be generated locally at the bow shock or in the magnetosheath.

Polar Cusps. Much of the present limited understanding of the processes in the cusp regions has been based on remote sensing measurements at medium and low altitudes. High-resolution multi-point *in situ* measurements at high altitudes across the magnetopause are needed to clarify the situation. In particular, it needs to be established how much of the plasma found in the cusp has entered locally and by what processes, and how much is simply in transit on its way from subsolar entry to the polar magnetosphere. Further theoretical work is needed to substantiate the existing largely qualitative models.

Boundary Layer Global Structure and Topology. Widely spaced multi-point measurements and imaging are needed to infer the global structure and its temporal variations as a function of the IMF. Such measurements will help distinguish between different transfer processes. For example, gradient drift entry of ions may occur primarily on the dawn side, while diffusion is expected to be widely distributed, and reconnection for southward IMF leads to entry along a swath emanating from an X-line located somewhere on the dayside. Macroscopic simulation studies in three dimensions are very useful as a guide in these investigations but should be complemented by microscopic simulations. Another still unresolved question concerns the topology of the LLBL, *i.e.* which part is located on open and which part is on closed field lines and how the topology depends on external or internal conditions, such as IMF direction and local magnetic shear.

Ion Composition Diagnostics. Composition measurements directly bear on the transfer mechanism across the magnetopause, but have so far not been made with sufficient time resolution to be conclusive. Detailed comparisons, for example of abundance ratios of solar wind ions across the magnetopause can be used to check for FLR effects and/or to establish how much particle reflection occurs. It is also important to remember that the fundamental conservation equations that form the basis of many of the tests described in this chapter involve the mass density of the plasma. In the absence of adequate mass-resolved measurements, assumptions about composition have had to be made.

Composition differences directly affect the diffusivity. Classical theory predicts slower diffusion for heavier particles at the same temperature. Because the overall diffusivity is ambipolar, the addition of heavy ions retards diffusion and thereby the entire plasma transport. In anomalous diffusion, it has been argued

that the relevant diffusion coefficient is proportional to the lower hybrid frequency. Since this decreases with mass, adding heavy ions to a plasma effectively reduces diffusion.